



Improving Linear Range Limitation of Non-Enzymatic Glucose Sensor by OH⁻ Concentration

By

Wenjuan Yang, B.Eng.

A Thesis

Submitted to the School of Graduate Studies

in Partial Fulfilment of Requirements

for the Degree

Master of Applied Science

© Copyright by Wenjuan Yang, Apr. 2020

MASTER OF APPLIED SCIENCE (2020)

McMaster University, Hamilton, Ontario

Faculty of Material Science and Engineering, Engineering Graduate Program

TITLE: Improving Linear Range Limitation of Non-Enzymatic. Glucose Sensor by OH⁻ Concentration

AUTHOR: Wenjuan Yang, B.S. (Taiyuan University of Technology)

SUPERVISOR: Dr. Gu Xu

COMMITTEE MEMBERS: Dr. Joe McDermid

Dr. Oleg Rubel

NUMBER OF PAGES: 74

ACKNOWLEDGMENTS

My supervisor, Dr. Gu Xu, fully funds this research. First, I am deeply grateful to my supervisor Dr. Gu Xu for his unforgettable encouragement, countless support and patience in my research work. He spares no effort to teach me not only about how to do research but also about how to be a better self. Thank you so much for offering me such a precious opportunity. I have learned a lot from you during this remarkable journey. Furthermore, as a group leader, he performs perfectly in unifying our group members and creating a family-like atmosphere among us. It is the harmonious ambiance established by Dr. Gu Xu that promotes me to progress during my research career. Thanks to Dr. Gu Xu.

Second, my colleagues in Xu's Research Group also helped me a lot in the past two years, and here I must extend my gratitude to Ryan T. Wang, Jason Y. Chen, Alex F. Xu, Edward G. Tai, and Elton E. Liu for their suggestions and assistance in my research.

Thirdly, I appreciate my committee members for their time and patience. And also, I want to give my appreciation to all the professors who have instructed me on the research and courses, the technicians, and staff who have helped me with my research.

Finally, I sincerely thank my family for their help and care, including my parents, my sister, and my brother. It was them who gave me endless happiness and gave me support both mentally and physically. Without them, my life in

Canada would be more difficult and colorless. Here, thanks very much for your concern during all these times, I must try my best to achieve my life goal.

Table of contents

1	INTRODUCTION.....	13
1.1	DIABETES AND GLUCOSE DETECTION	13
1.2	GLUCOSE MONITORING BY ELECTROCHEMICAL MOTHED.....	16
1.2.1	<i>The enzymatic glucose sensor.....</i>	<i>17</i>
1.2.2	<i>The non-enzymatic glucose sensor.....</i>	<i>25</i>
2	EXPERIMENTAL.....	32
2.1	MATERIALS	32
2.2	NI (OH) ₂ /NI FOIL ELECTRODE PREPARATION	32
2.3	MATERIALS CHARACTERIZATION	33
2.4	ELECTROCHEMICAL PROPERTIES MEASUREMENTS	33
2.5	FTIR SPECTRA MEASUREMENTS	34
2.6	UV–VIS SPECTRA MEASUREMENTS.....	35
2.7	NMR SPECTRA MEASUREMENTS.....	35
3	RESULTS AND DISCUSSION	36
3.1	X-RAY DIFFRACTION (XRD) MEASUREMENT OF NI(OH) ₂ /NI SHEET	36
3.2	ELECTROCHEMICAL CHARACTERIZATIONS.....	37
3.2.1	<i>Electrochemical reaction.....</i>	<i>37</i>
3.2.2	<i>Cyclic voltammetry (CV) analysis of Ni(OH)₂.....</i>	<i>38</i>
3.2.3	<i>Effect of scan rate.....</i>	<i>39</i>
3.2.4	<i>Amperometric investigations.....</i>	<i>40</i>
3.2.5	<i>Anti-interference ability.....</i>	<i>45</i>
3.3	FTIR TEST	46
3.4	UV AND NMR TEST.....	48

4	CONCLUSION	51
5	REFERENCE.....	52

List of Figures

Figure. 1 Number of diabetic patients worldwide(International Diabetes Federation., 2017)	14
Figure. 2 Healthcare costs for people with diabetes(da Rocha Fernandes et al., 2016)	15
Figure. 3 Commercial glucometer for diabetes monitoring(Liberman et al., 2011)	16
Figure. 4 Glucose oxidase (GOx) molecule showing the FAD cofactor embedded within the protein matrix(Wilson and Elizabeth, 2016)	18
Figure. 5 FAD/ FADH ₂ redox couple conversion reaction(Liu et al., 2008)	18
Figure. 6 Schematic diagrams of the 1 st generation enzymatic glucose sensors	19
Figure. 7 The original YSI serum-glucose biosensor for diabetes clinics 1975(Turner, 2014)	21
Figure. 8 Schematic diagrams of the 2 nd generation enzymatic glucose sensors	23
Figure. 9 Schematic diagrams of the 3 rd generation enzymatic glucose sensors	25
Figure. 10 Schematic diagram of the 4 th generation non-enzymatic glucose sensors (Liu et al., 2005; Wani et al., 2016; Zayats et al., 2002)	26
Figure. 11 Diagram of the number of recent publications on non-enzymatic glucose sensors as a function of the year published(Zhu et al., 2016)	28
Figure. 12 relationships between concentration and current response (Gonzales et al., 2019)	29
Figure. 13 Schematic diagram of working electrode non-enzymatic glucose sensors	34
Figure. 14. X-ray diffraction (XRD) results (WL = 1.54 Å) for Ni (OH) ₂ on the Ni sheet; ▼:Ni(OH) ₂ ; ○: Ni sheet.	36
Figure. 15 The schematic diagram shows how both oxidative and reductive reactions are catalyzed at the working electrode surface	38

- Figure. 16 (a) The CV curve in 100mM NaOH solution; (b) the CV curve in 500mM NaOH solution; (c) the CV curve in 1000mM NaOH solution; (d) schematic illustration of the Cyclic Voltammetry measurement apparatus 39
- Figure. 17 (a) CV responses of Ni(OH)₂/NiOOH electrode in the presence of 1mM glucose in 500mM NaOH solution under various scan rates; (b) the relationship between the current and scan rate. 40
- Figure. 18 (a) The amperometric I-t curve at [OH⁻]=100 mM; (b) the amperometric I-t curve at [OH⁻] = 1000 mM; (c) the amperometric I-t curve at [OH⁻] = 500 mM; the linear range concentration of glucose at various OH⁻ concentrations, (d) [OH⁻] = 100 mM, (e) [OH⁻] = 500 mM and (f) [OH⁻] = 1000 mM. 41
- Figure. 19 The relationship between electrolyte solution concentration and upper linear range of detection glucose 42
- Figure. 20 (a) Current responses of the Ni(OH)₂/Ni sheet electrode after adding 1 mM glucose following by the injection of 1 mM LA, AA, urea, sodium citrate, galactose, fructose, sodium benzoate and L-cysteine with 35 s intervals into stirring 1 M NaOH solution at the constant potential of +0.5 V (vs. Ag/AgCl), respectively, (b) Column chart for the comparison between the response of the electrode toward 1 mM glucose against 0.1 mM LA, AA, urea, sodium citrate, galactose, fructose, sodium benzoate and L-cysteine. 46
- Figure. 21 (a) Fourier-transform infrared spectroscopy (FTIR) results of glucose/NaOH mixture; (b) FTIR results of a pure glucose electro-oxidized product and glucose/NaOH electro-oxidized mixture were measured by FTIR. 47
- Figure. 22 UV-vis spectra of the glucose/NaOH mixture solution (solid line) and glucose solution (dash line). 48
- Figure. 23 ¹³C DEPTQ-135 NMR spectrum of glucose/NaOH mixture dissolved in D₂O with a frequency of 125.78 MHz. 49

List of Tables

table 1. The relationship between the linear range and the alkaline concentration of various non-enzymatic glucose sensors.

43

List of Abbreviations

DM	diabetes mellitus
IDF	International Diabetes Federation
GOx	enzyme- oxidase
FAD	flavin adenine dinucleotide
CGM	continuous glucose monitoring
mmol/L	mM
SCE	Saturated calomel electrode
LOD	limit of detection
rGO	reduced graphene oxide
GCE	glassy carbon electrode
CNTs	carbon nanotubes
SPCE	screen-printed carbon electrode
LA	lactic acid
AA	ascorbic acid
FTIR.	Fourier-Transform Infrared Spectroscopy

NMR Nuclear Magnetic Resonance Spectroscopy

CV Cyclic Voltammetry

Abstract

To combat diabetes mellitus(DM), a chronicle metabolic disease, from which more than 400 million people suffered in the world, the patients must check the blood glucose level 4-5 times daily with an enzyme-based blood glucose meter and adjust blood glucose levels accordingly. The problem is that enzymatic glucose meters become unstable in the tropics. Therefore, the non-enzymatic method has been urged for blood glucose monitoring, among which the transition metal oxide electrode was found to be promising. However, despite the prolonged effort, its linear detection range is usually much smaller than the glucose level of diabetic patients, calling for an effective solution. Despite many previous attempts, none have solved the problem. Such a challenge has now been conquered by raising the NaOH concentration in the electrolyte, where amperometry, X-ray diffraction, Fourier-transform infrared spectroscopy, and Nuclear magnetic resonance measurements have been conducted. The linear range has been successfully enhanced to 40 mM in 1000 mM NaOH solution, and it was also found that NaOH affected the degree of glucose oxidation, which influenced the current response during sensing. It was expected that the alkaline concentration must be 25 times higher than the glucose concentration to enhance the linear range, much contrary to prior understanding.

1 Introduction

1.1 Diabetes and glucose detection

Diabetes mellitus is a chronic metabolic disease in which the human body cannot produce or respond to the hormone insulin, resulting in abnormal blood glucose levels(Chen et al., 2019; O’Connell et al., 2006; Renard, 2005; Risérus et al., 2009). It may cause severe complications including blindness, kidney failure, heart attack, stroke, and lower limb amputation, etc.(Liu et al., 2019; O’Connell et al., 2006; Turner, 1998; UK Prospective Diabetes Study Group, 1998; Van Den Berghe et al., 2006). According to the International Diabetes Federation(IDF) currently, as shown in **Figure.1**, there are 463 million adults aged from 20 to 79 years old (9.3% of the population) with diabetes, which means that 1 in 11 adults is with diabetics(International Diabetes Federation., 2017; Risérus et al., 2009). Furthermore, it’s estimated that more than 550 million people worldwide will have diabetes by 2030, and the number is expected to increase by 55% for the next 25 years(Brauker, 2009; Tamborlane et al., 2008). Based on the data provided by the IDF, about 5 million deaths were attributed to diabetes in 2014 alone, which will be the 7th lethal disease in 2030(Hwang et al., 2018; Liu, 2006; Park et al., 2006).

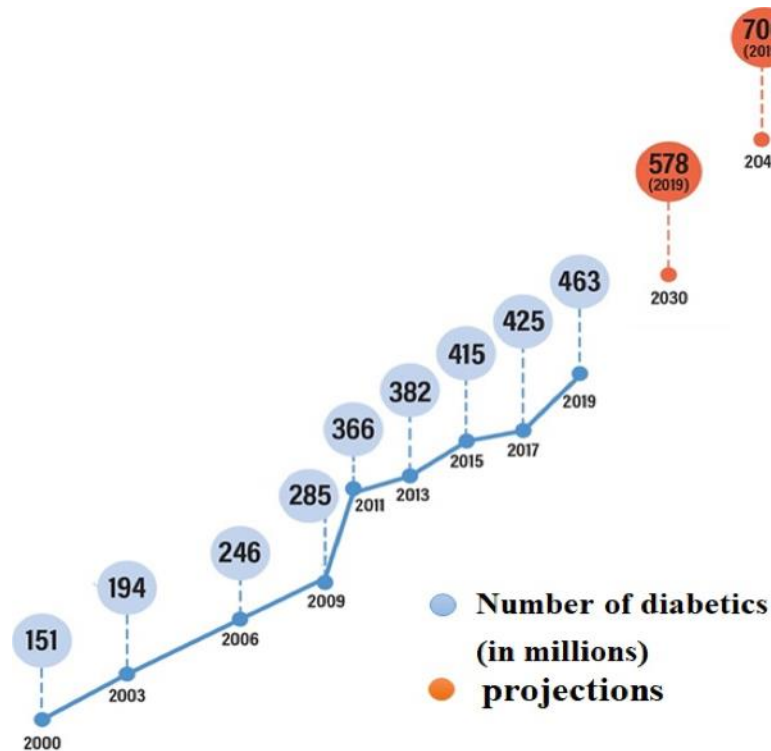


Figure. 1 Number of diabetic patients worldwide(International Diabetes Federation., 2017)

Moreover, according to IDF, in **Figure.2**, it demonstrated that global diabetes healthcare spending had increased by 79%, from 362 billion USD in 2009 to 673 billion USD in 2015(12% of total expenditures on global healthcare) and was projected that spending on diabetes control and treatment would increase to 802 billion USD in 2040. This increasing figure showed that diabetes would impose a substantial economic burden on society(Cho et al., 2018; da Rocha Fernandes et al., 2016; Whiting et al., 2011).

12% of global healthcare expenditure was for diabetes in 2015

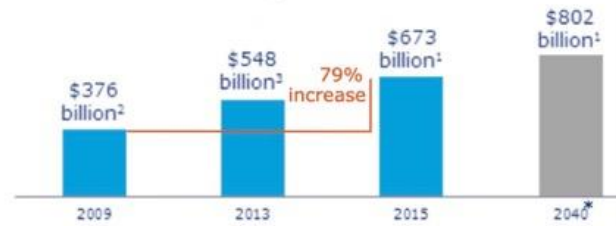
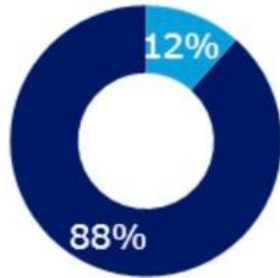


Figure. 2 Healthcare costs for people with diabetes(da Rocha Fernandes et al., 2016)

Recent researches have shown that the risk of mortality and of complications in people with diabetes can be reduced through strict sugar control(Cho et al., 2018; Luo et al., 2012; Raveendran et al., 2017; Zhuang et al., 2008). As such, regular monitoring of blood glucose levels and reducing budgets are of great importance in fighting against diabetes and preventing those complications, and the patients must puncture their fingers 5–7 times every day to monitor the blood glucose level via enzyme-based glucose test-strips, which currently dominate the market. (Cha and Meyerhoff, 2017; Chase et al., 2010; Yadav et al., 2015)



Figure. 3 Commercial glucometer for diabetes monitoring(Liberman et al., 2011)

1.2 Glucose monitoring by electrochemical method

The detection technology which measures the concentration of glucose is thought of as the vital component of a glucose monitoring device. Over the last four decades, in order to modify the performance of this technology, huge amount of effort has been made. Since the enzymatic electrode was first invented in 1962 by Clark and Lyons, an increasing number of researchers have paid attention to developing and improving biosensors for practical application(Hwang et al., 2018; Park et al., 2006; Toghil and Compton, 2010; Yoo and Lee, 2010).

There are many reports on the improvement of blood glucose sensors. In general, the development of electrochemical glucose sensors can be divided into four generations (Alwarappan et al., 2009; Park et al., 2006; Wu et al., 2012; Zhang and Chen, 2017; Zhang and Li, 2004). Actually, the first three generations are enzymatic glucose sensors; while the fourth generation is non-enzymatic glucose sensors (Putzbach and Ronkainen, 2013; Wang et al., 2013).

1.2.1 The enzymatic glucose sensor

The enzyme-oxidase (GOx), which was the crucial catalytic component, was immobilized on the enzymatic electrode (Gonzales et al., 2019; Tremey et al., 2014). Actually, Wilson and Turner described the GOx as the "ideal enzyme" for glucose oxidation in a 1992' review because of its excellent performance, such as high sensitivity and good selectivity (Wilson and Elizabeth, 2016). Glucose oxidase (GOx) molecule is shown in **Fig. 4**. The redox center flavin adenine dinucleotide (FAD) is the core component of this huge protein molecule and protected by a thick protein matrix (Editor, n.d.; Fajardo et al., 2016). Usually, as shown in **Fig. 4**, FAD, existing in the form of quinone, gains electrons, and is reduced to FADH₂ (living in the form of hydroquinone when it interacts with glucose (Toghill and Compton, 2010). Besides, glucose also is oxidized to gluconolactone, in accordance with **Fig. 5** (Chen et al., 2013).

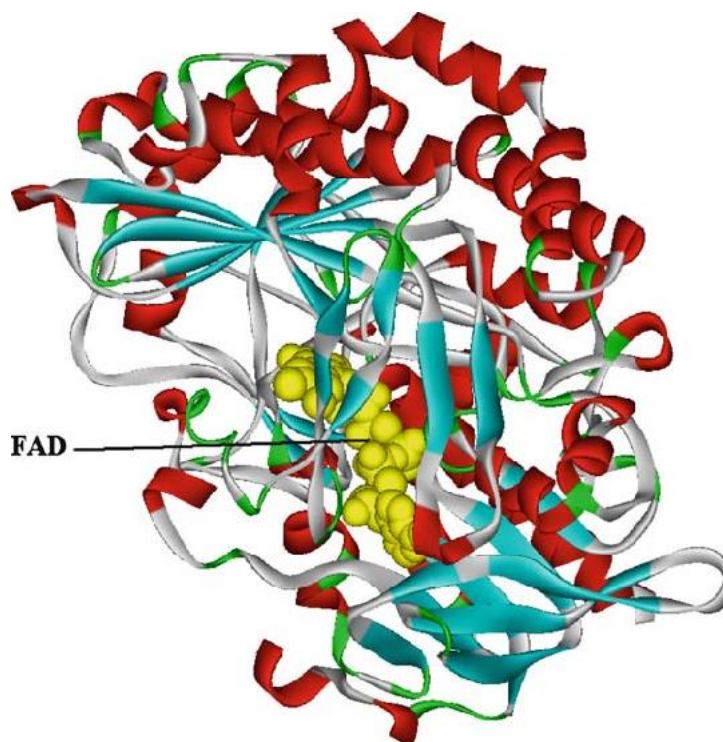


Figure. 4 Glucose oxidase (GOx) molecule showing the FAD cofactor embedded within the protein matrix(Wilson and Elizabeth, 2016)

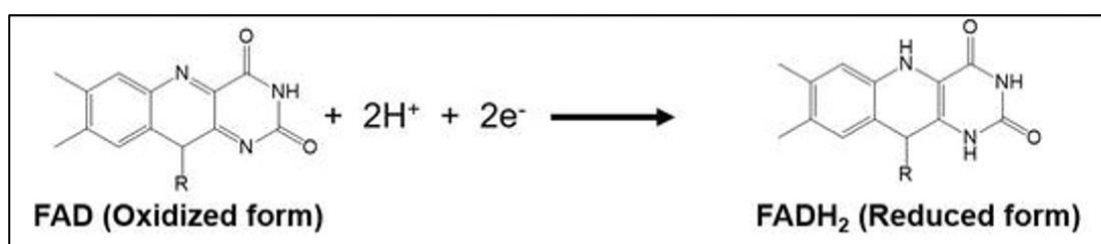


Figure. 5 FAD/ FADH₂ redox couple conversion reaction(Liu et al., 2008)

1.2.1.1 The 1st generation glucose sensor

In fact, because FAD is located deep in GOx and surrounded by a thick protein layer, electron transfer between the electrode and the active centre becomes the main factor limiting glucose detection(Liu et al., 2008; Wilson and Elizabeth, 2016).

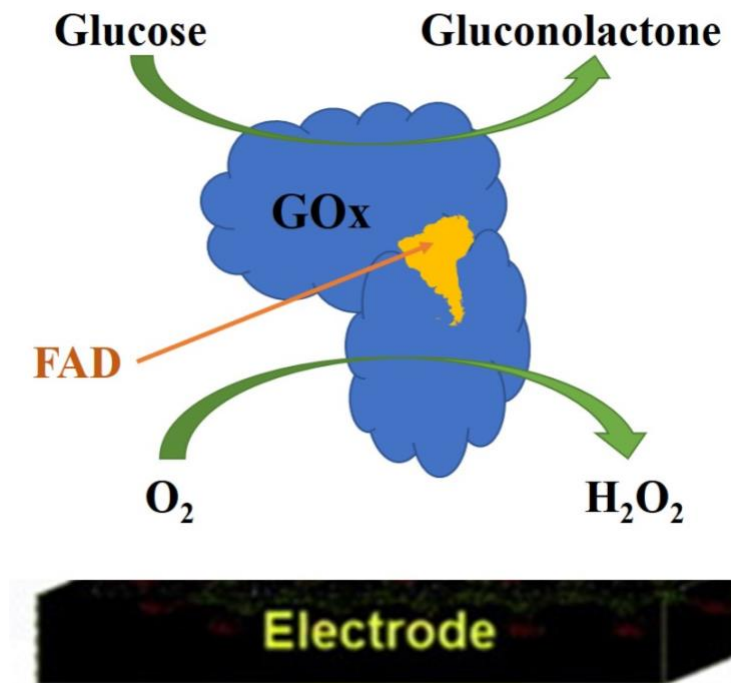


Figure. 6 Schematic diagrams of the 1st generation enzymatic glucose sensors

As shown in **Fig. 6**, in the first-generation glucose sensors, oxygen was used as an electron mediator between enzyme(GOx) and the electrode surface. The mechanism of the 1st enzyme sensor is as follows: when glucose was present, GOx oxidized glucose to gluconolactone and FAD was reduced to FADH₂, and next dissolved oxygen oxidized FADH₂ to generate hydrogen peroxide and FAD

which was used to oxidized glucose(Besteman et al., 2003; Liu, 2006; Liu et al., 2008; Park et al., 2006). Therefore, the generation rate of hydrogen peroxide or the consumption rate of oxygen is directly proportional to the glucose concentration that can be determined by an increase in hydrogen peroxide or a decrease in oxygen(Malitesta et al., 1990). The first commercial glucose biosensor fabricated by the Yellow Spring Instrument Company in 1975 (**Fig. 7**) used this mechanism(Turner, 2014). Owing to its high cost of the working electrode (Pt), the application of this amperometric glucose detector was limited and only used for glucose measurement clinical laboratories(Wang et al., 2020; Xu et al., 2019).

However, the most essential problem of first-generation glucose sensors is insufficient oxygen(Wang et al., 2000). In detail, there is not sufficient dissolved O₂ in the real blood to make sure that glucose can be efficiently oxidized so that blood glucose levels can't be detected accurately when O₂ is deficient(Toghill and Compton, 2010). Although many approaches had been proposed, including the use of specific films that allow more O₂ passing through the film and using an oxygen-rich material as an electrode to increase the reactive O₂(Armour et al., 1990; Kashyap and Lu, 1998). But these methods need a more complicating fabrication approach and enlarge the overall sensor volume.



Figure. 7 The original YSI serum-glucose biosensor for diabetes clinics 1975(Turner, 2014)

1.2.1.2 The 2nd generation glucose sensor

Fig. 8 depicts the usual structure of the 2nd generation glucose monitor. This type of sensor replaced O_2 (electron mediator of 1st generation glucose sensor) with artificial mediators to solve the problem brought by oxygen deficit in the real measured sample(Newcomer, 2005; Scheller et al., 1991). In second-generation glucose sensors, small redox-active molecules such as ferrocene derivatives, ferrocyanide, conductive organic salts and so on, were used as electron mediators. These mediators improved the electron transfer rate between the FAD (redox center of the active site of the enzyme) and the electrode surface through a fast and reversible redox reaction(Harper and Anderson, 2010; Nagata et al., 1995; Shim et al., 2009; Yu et al., 2003; Zhang et al., 2005). In fact, on the electrode surface, redox mediators instead of oxygen are used to oxidize $FADH_2$.

Then this mediator was oxidized on the electrodes to generate a monitorable current signal and redox mediators were regenerated(Cui et al., 2001).

Unfortunately, there are some problems still existing in the second-generation sensors. Firstly, it's quite difficult to keep the mediator near the enzyme and electrode surface since the small molecules are diffusive, which is terrible for prolonged use and requires more complicated and elaborate ways to tether the mediator between enzyme and electrode(Gorton et al., 1991). Secondly, although the reaction rate between enzyme and mediator is faster than that of O₂; dissolved oxygen is also complete with the mediator, which reduces the accuracy of the system(Toghill and Compton, 2010). Furthermore, the mediator may also oxidize the other interference species, which further decreases the accuracy and efficiency(Wang, 2001).

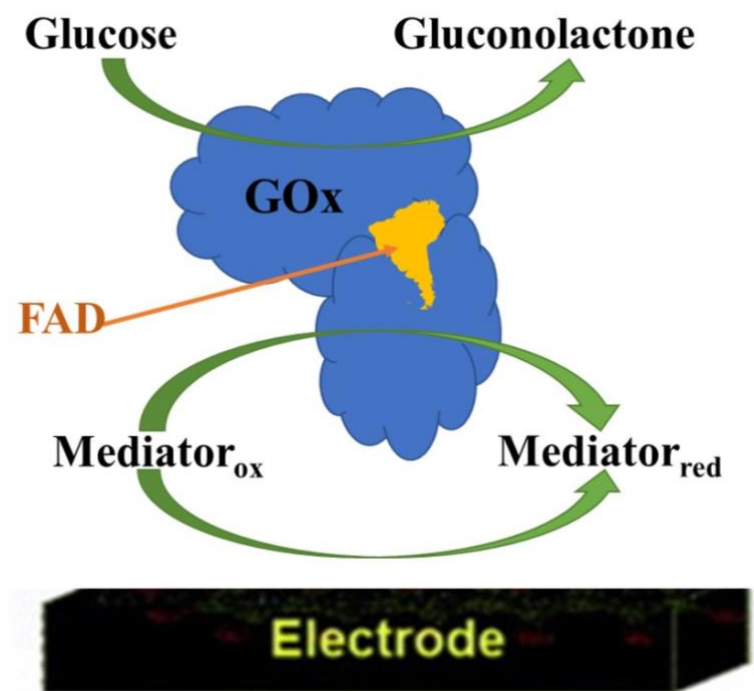


Figure. 8 Schematic diagrams of the 2nd generation enzymatic glucose sensors

1.2.1.3 The 3rd generation glucose sensor

As shown in **Fig. 9**, in the third-generation glucose sensors, there is no need for natural or artificial mediators between the redox centre of the active site of the enzyme and electrode, and electrons can be transferred between them directly (Karunakaran et al., 2015). Although it was an ambitious idea, the mediator-free glucose sensor was realistic due to the development of nano and porous materials (Viet et al., 2018). Originally, the biggest problem for direct electron transfer between the electrode and enzyme is the existence of thick protein in which the redox sites are embedded (Chen et al., 2014; Wang and Lee, 2015; Wang, 2001; Zhai et al., 2013). However, currently, electrically wiring the electrode and the active redox sites of the enzyme or using porous materials as

the working electrode that could help entrap and encompass the protein, could realize the direct electron transfer between the electrode and enzyme(Chaubey and Malhotra, 2002; Habermüller et al., 2000; Kang et al., 2009; Léger et al., 2003).

The most valuable point of this system is the successful elimination of possible interferences and transforms the enzymatic recognition events of glucose to amperometric signals directly irrespective of the concentration of oxygen or redox mediators(De Poulpiquet et al., 2014; Freire et al., 2003; Martins et al., 2014; Pumera et al., 2007). In summary, this new system would avoid the complications of tailored mediators and improve selectivity and sensitivity. By this strategy, Gooding and co-workers electrically connected enzyme and electrode by exploiting carbon nanotubes to connect the active site of apo-GOx to the electrode surface(Liu et al., 2005).

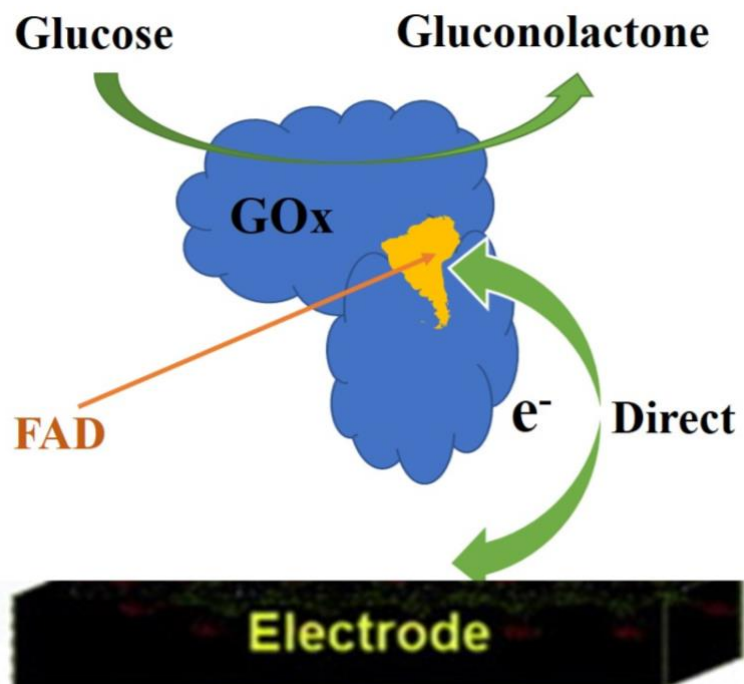


Figure. 9 Schematic diagrams of the 3rd generation enzymatic glucose sensors

1.2.2 The non-enzymatic glucose sensor

In the fourth-generation glucose sensors, the enzyme used in those three former-generation sensors would be replaced by nano or porous materials as catalysts, called non-enzymatic sensors.

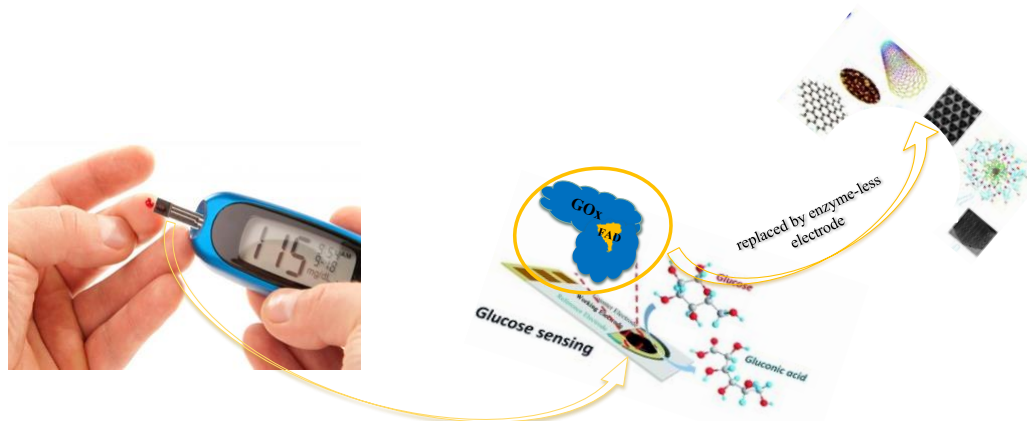


Figure. 10 Schematic diagram of the 4th generation non-enzymatic glucose sensors (Liu et al., 2005; Wani et al., 2016; Zayats et al., 2002)

The stability problem is the leading and most serious problem of traditional enzyme sensors, which derives from the inherent characteristics of enzymes (Spanning and Neujahr, 1990; Yadav et al., 2015). Enzyme-based glucose sensors are difficult to get rid of deformations, including thermal or chemical deformation, during their fabrication, packing, storing, and use. In detail, when the temperature is higher than 40 °C or pH < 2 and pH > 8 could cause severe damage to the sensor. Besides, storing or in-use sensors would also be damaged by high or low humidity (Gupta et al., 2013; Spanning and Neujahr, 1990; Wang et al., 2011; Zhuo et al., 2011). Therefore, because of the intrinsic shortcomings of enzymes, non-enzymatic glucose sensors have entered the field of vision of researchers in recent years (Bernards et al., 2008; Cherevko and Chung, 2009; Li et al., 2013; Rolland et al., 2006). As we all know, non-enzymatic glucose sensors can be free from restrictions such as temperature,

humidity, solvents, and manufacturing processes(Hwang et al., 2018; Park et al., 2006). Hence, establishing a dependable mass production process would become easier. More importantly, traditional subcutaneous enzymatic glucose sensors need to sterilize during the entire manufacturing line, while the non-enzymatic blood glucose sensors need to be sterilized only before packaging, which decreases manufacturing costs(Bruen et al., 2017; Niu et al., 2016). This advantage of enzyme-free sensors is expected to reduce significantly the unit price of a continuous glucose monitoring system (CGM system)(Oliver et al., 2009; Vashist, 2013; Wang et al., 2010).

As shown in **Figure.11**, the number of publications in the field of enzyme-free glucose sensors has been demonstrated in the past 15 years, and the number of publications has increased dramatically from 2001 to 2015, indicating an increasing number of researchers in the development(Zhu et al., 2016)

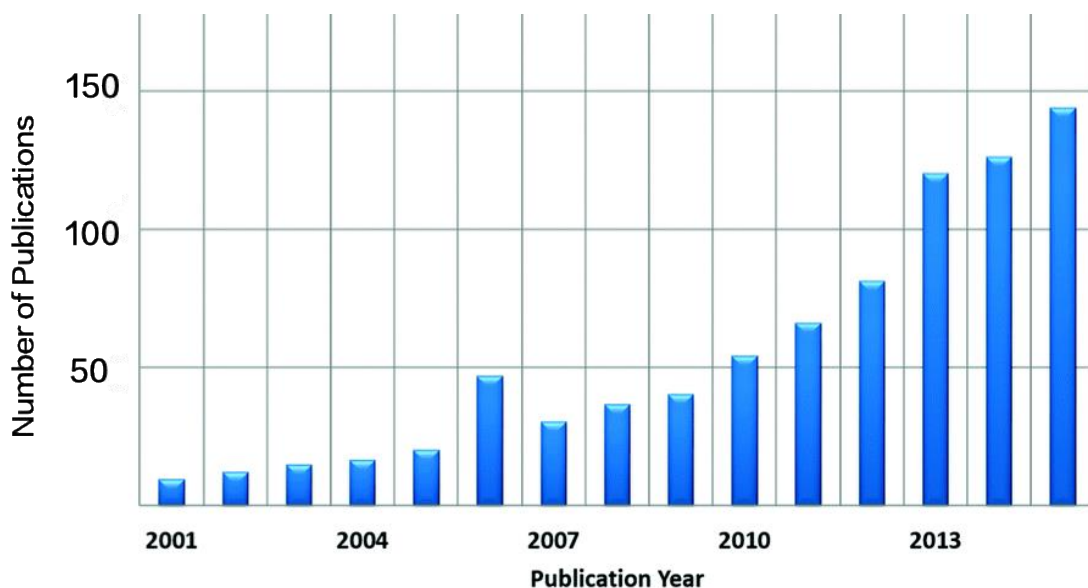


Figure. 11 Diagram of the number of recent publications on non-enzymatic glucose sensors as a function of the year published(Zhu et al., 2016)

Although non-enzymatic glucose sensors show many advantages, their detection range is limited to up to several mmol/L(mM), which is much smaller than the blood glucose levels of patients with diabetes (1–30 mM)(Dong et al., 2018; Jia et al., 2018; Kim et al., 2018; Song et al., 2010; Zang et al., 2018). As shown in **Fig.12**, when measuring glucose concentration, the current response first enters a linear range within which a linear relationship between the current response and the glucose concentration can be expected(Hwang et al., 2018; Shadlaghani et al., 2019). Next, a non-linear relationship is observed in a region called the non-linear range in which the relationship between the current response and the glucose concentration is unpredictable(Shadlaghani et al., 2019). Eventually, the current reaches the saturation point, beyond which the current response begins to decrease.

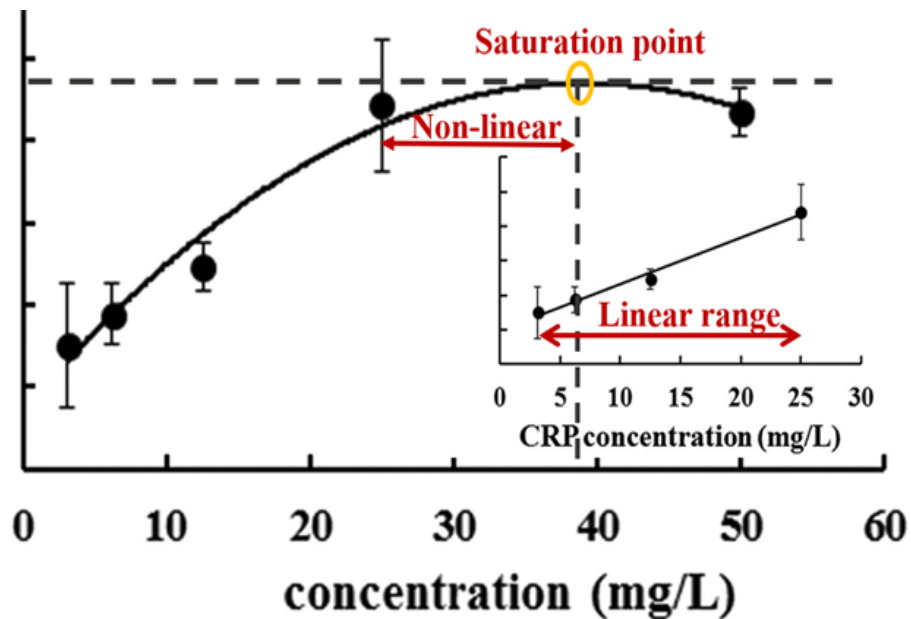


Figure. 12 relationships between concentration and current response (mmol/L=18mg/L) (Gonzales et al., 2019)

In the linear detection range, the glucose levels can be easily calculated from linear relationships between the current signal and glucose concentration. We all know that although current can increase in a non-linear range (that is, between a linear range and a saturation point), as blood glucose levels rise, the range is useless because saturation is not fixed (Chinnadayyala et al., 2018; Wang et al., 2015). Therefore, only the linear range is meaningful for patients to measure blood glucose levels. We can only calculate glucose concentration based on the current response in the linear range, which leaves a challenge to improving the linear range (Hwang et al., 2018).

Many techniques have been tried to improve the linear range. Some researchers believed that the linear range was restricted by the working potential

(Annalakshmi et al., 2019). By changing the ratio of Pt, Ni, and Co metal elements, the working potential was adjusted from 0.45 V vs. Saturated calomel electrode (SCE) to 0.4 V vs. SCE. Still, the linear range of the measurement was basically unchanged (from 1.5 μM – 8 mM to 1 μM –8.5 mM)(Mahshid et al., 2013). On the other hand, others believed that the problem was mainly related to the specific surface area of the electrode(Ding et al., 2011; Pradhan et al., 2010; Rong et al., 2007; Yuan et al., 2005). Mian Li et al. synthesized a 3D nanostructured electrode with a large specific surface area, but the linear range (50 μM –8 mM) did not increase to any appreciable level(Li et al., 2014). This suggests that the reason of the limited linear range must be found form an effective strategy, as all the blind trials have not been able to solve this problem.

It was, therefore, the purposes of the current research to find the factors that limited the linear range and extend the range to the required level. Among electro-catalysts used in enzyme-free glucose sensors, metal oxides possess certain outstanding advantages for this application, e.g., low cost, controllable synthesis, functional biocompatibility, chemical stability, so that we took the Ni(OH)₂ as an example and employed amperometry, Fourier-Transform Infrared Spectroscopy (FTIR), and Nuclear Magnetic Resonance Spectroscopy(NMR). Eventually, it is found that the hydroxide ion concentration affects the linear measurement range, and the ion concentration must be 25 times higher than the glucose concentration. In detail, the higher OH level could promote the conversion of glucose to enediol, which lowered the energy barrier of the subsequent electrooxidation reaction, so that more than four electrons were transferred to the counter electrode. Meanwhile, the final product was glucuronic acid instead of gluconolactone, which would increase the current response and

the linear range to 40 mM. Therefore, the real cause we have revealed for the limited linear range can not only promote a conceptual understanding of the working mechanism of non-enzymatic glucose sensors but also distinguish various assumptions and conflicts. Hopefully, these discoveries are able to improve sensor performance and accelerate their commercialization.

2 Experimental

2.1 Materials

NaOH pellets (ACS reagent, $\geq 99.0\%$) were purchased from E-Merck. Dextrose (99.0%, SRL, India) and 5 wt% Nafion solution (Sigma-Aldrich) were adopted for all electrochemical analyses. Deionized water (DI water) (Molecular Biology Reagent, purchased from Sigma-Aldrich, Mississauga, ON, Canada) ethanol (95.0%, Sigma-Aldrich, Mississauga, ON, Canada) and acetone(95.0%, Sigma-Aldrich, Mississauga, ON, Canada) were adopted as the solvents. Ni $(\text{NO}_3)_2 \cdot 6\text{H}_2\text{O}$, KBr, Ni sheet (0.05 m thick), and D_2O (analytical reagent grade) were purchased from Sigma-Aldrich.

2.2 Ni $(\text{OH})_2$ /Ni foil electrode preparation

Firstly, Ni $(\text{OH})_2$ powders were synthesized according to the precipitation method reported in the literature.(Yang et al., 2014). Concentrated sodium hydroxide solution was dropped into 1mol/L Ni $(\text{NO}_3)_2$ solution. The precipitation reaction was at 45 with stirring (700rpm). The resulting green precipitate of Ni $(\text{OH})_2$ powders were filtered, dried, and washed with DI water several times to remove possible impurities. Although it is possible to further detect the impurities by, e.g., EDS, XPS, etc., this becomes unnecessary in our case, as the possible impurities will not be involved in the voltage range, causing any errors here. The precipitate was dried in air. Subsequently, Homogeneous suspension of Ni $(\text{OH})_2$ samples was gained by sonicating the powder in several

drops of ethanol. Then the suspension was dropped on the Ni foil electrode, after which 0.5% Nafion binder solution was placed on the sample layer to fix the material on Ni foil. Finally, the electrode was air-dried before the measurements.

2.3 Materials characterization

The sample (Ni (OH)₂ powders) was characterized by powder XRD (Bruker D8 DISCOVER diffractometer) with CuK α 1 radiation ($\lambda = 1.54 \text{ \AA}$)

2.4 Electrochemical properties measurements

The three-electrode electrochemical cell was used to monitor glucose levels. Ag/AgCl (saturated KCl solution) was used as a reference electrode, although some reference electrodes would be affected by alkaline electrolyte such as Saturated calomel electrode (SCE); Ag/AgCl reference electrode is stable in the alkaline electrolyte (Elgrishi et al., 2018). Ni (OH)₂ / Ni sheet was used as working electrode, and Au wire was the counter electrode. All the measurements were carried out on a CMS100 electrochemical workstation (purchased from The Illinois Department of Central Management Services) at room temperature. Before the amperometry test, 150-cycle Cyclic Voltammetry (CV) analyses were conducted with cyclic voltage between 0.00 and +0.7V and a scan rate of 50 mV/s, where 100mM, 500mM and 1000mM NaOH solution used as background electrolyte, respectively. Then Amperometry I-t responses at an applied potential of +0.55 V (for 0.1mM NaOH solution) and +0.5 V (for 0.5M and 1M NaOH solution) were recorded under stirring at 350 rpm. The area of Ni (OH)₂ on Ni

sheet was $1.2 \times 0.15 \text{ cm}^2$. The surface area of electrode is $0.18 \text{ cm}^2 (1.2 \times 0.15 \text{ cm}^2)$

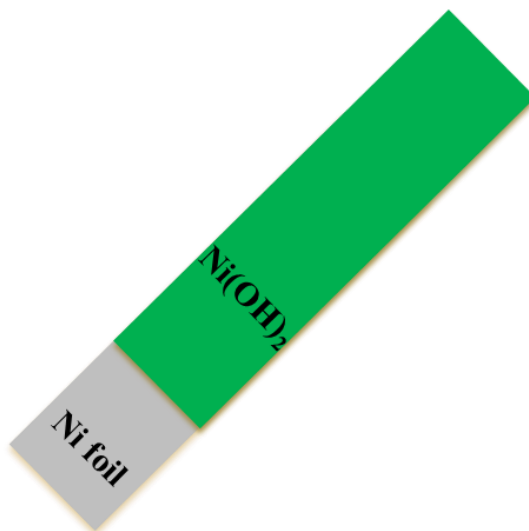


Figure. 13 Schematic diagram of working electrode non-enzymatic glucose sensors

2.5 FTIR spectra measurements

Glucose solution, glucose/sodium hydroxide mixed solution, glucose electro-oxidized solution, and glucose/sodium hydroxide electro-oxidized solution were dried by VirTis Bench Top Pro freeze-dryer (purchased from SP Scientific) to obtain powders. Then these powders were dispersed over dry KBr powder to prepare sample pellets for FTIR. Finally, the four samples were measured by a Nicolet 6700 FT-IR spectrometer to acquire the FTIR spectra in the wavenumber range of $400\text{--}4000 \text{ cm}^{-1}$ with a resolution of 1 cm^{-1} in DRIFT mode.

2.6 UV–vis spectra measurements

UV-vis measurements to glucose solution and mixed glucose solution were conducted on a DU800 Spectrophotometer. First, preheat the spectrophotometer for approximately 15 minutes. Second, fill the quartz cuvette with DI water as background to obtain the blank data. Third, remove the blank sample and rinse the cuvette with a small amount of fully mixed glucose solution (a drop of sample to per 100 ml DI water) until the cuvette was $\frac{3}{4}$ full. Finally, place the cuvette into the spectrophotometer, close the sample door and record the absorbance on the datasheet. The treatment to the mixed glucose solution is the same as above.

2.7 NMR spectra measurements

Glucose/NaOH mixture was dissolved in 0.6 ml D₂O. ¹³C NMR was recorded on Bruker DRX-500 MHz spectrometer with the frequency of 125.78MHz at room temperature and analyzed by Bruker Topspin 3.1 software.

3 Results and Discussion

3.1 X-ray diffraction (XRD) Measurement of Ni(OH)₂/Ni Sheet

The working electrode was characterized first by XRD, which confirmed the formation of Ni(OH)₂ on the Ni sheet, as demonstrated in **Figure.14**.

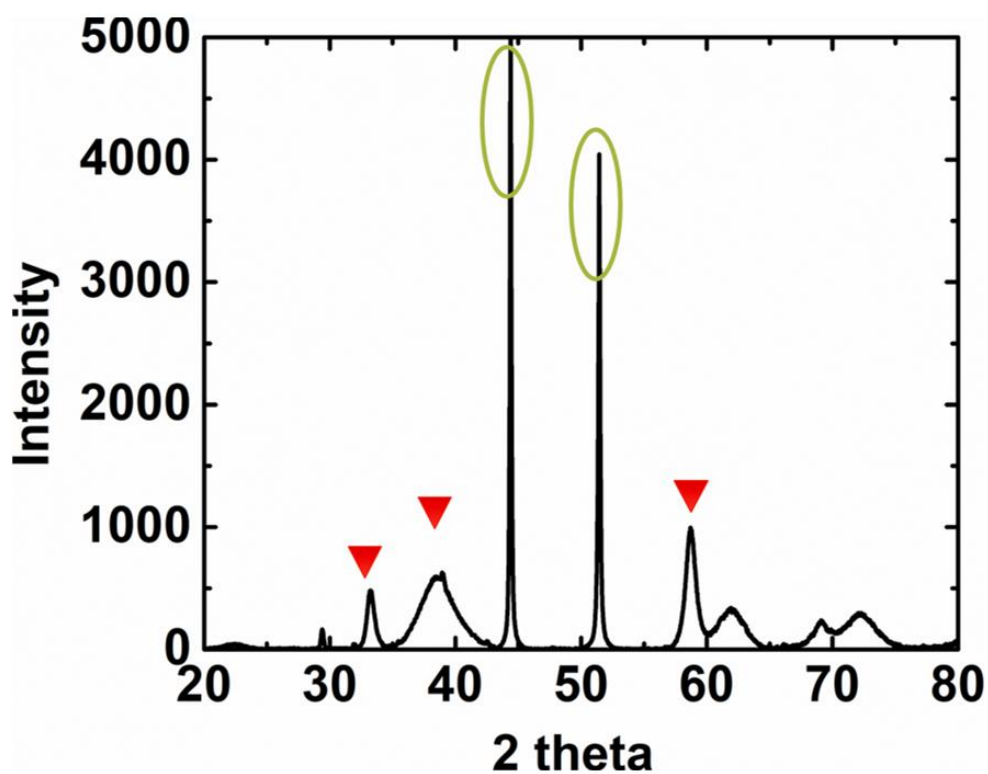


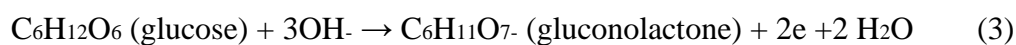
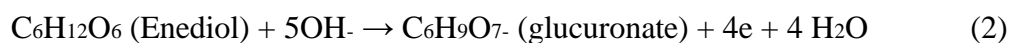
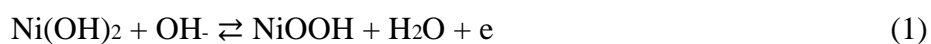
Figure. 14. X-ray diffraction (XRD) results (WL = 1.54 Å) for Ni (OH)₂ on the Ni sheet; ▼:Ni(OH)₂; ○: Ni sheet.

3.2 Electrochemical Characterizations

3.2.1 Electrochemical reaction

In the triple-electrode cell, complex electrochemical reactions took place, ad outlined below.

For the working electrode:



For the counter electrode:



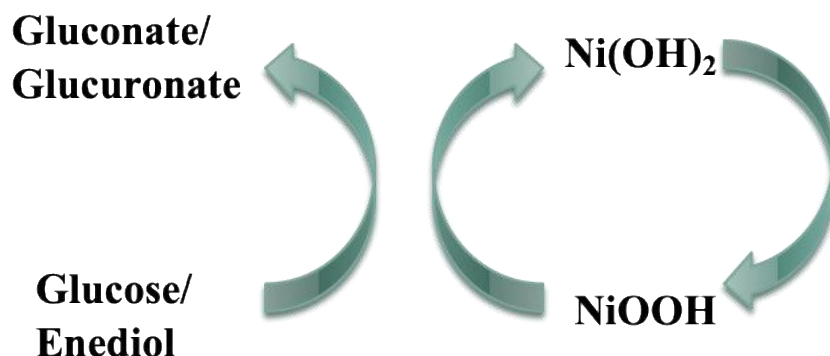


Figure. 15 The schematic diagram shows how both oxidative and reductive reactions are catalyzed at the working electrode surface

3.2.2 Cyclic voltammetry (CV) analysis of Ni(OH)₂

The electrode should be stabilized before making preliminary measurements. This can be achieved by continuously performing CV measurements in a 100/500/1000 mM NaOH solution at a scan rate of 50 mV / s (Wu et al., 2010). As shown in **Figure. 16** (a) (b) and (c), the CMS electrochemical workstation triggered a redox conversion between Ni(OH)₂ and NiOOH. When the current response reaches a maximum, the redox conversion stabilizes, indicating that equilibrium is being achieved. The current generated in a 100 mM NaOH solution varied between -1.8 to 2.4 mA and expanded to -2.9 to 3.5 mA in a 500 mM NaOH solution. This range was further extended to -3.5 to 5 mA in a 1000 mM NaOH solution. At higher base concentrations, a significant increase in the current response can be expected, which indicates that the base enhances the catalytic effect of the NiOOH / Ni(OH)₂ electrode, which is beneficial for glucose sensing.

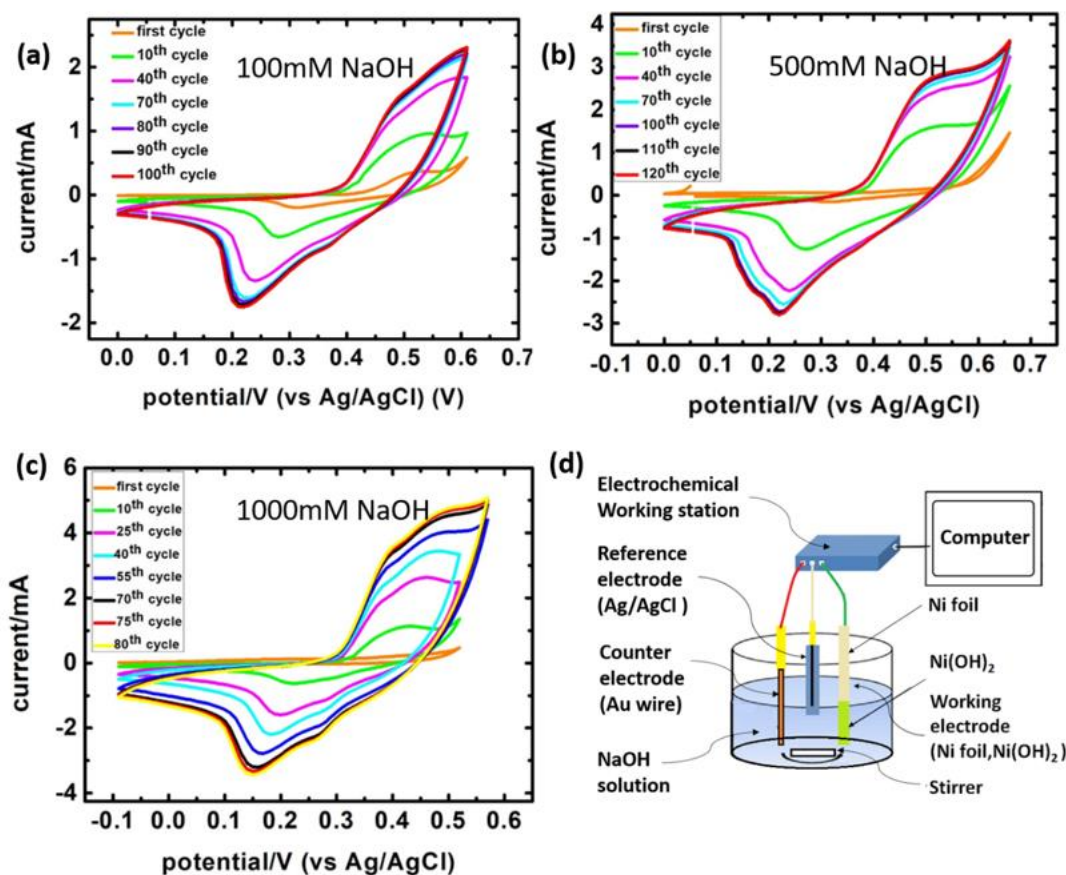


Figure. 16 (a) The CV curve in 100mM NaOH solution; (b) the CV curve in 500mM NaOH solution; (c) the CV curve in 1000mM NaOH solution; (d) schematic illustration of the Cyclic Voltammetry measurement apparatus

3.2.3 Effect of scan rate

The reaction type of glucose in the electrolyte should be investigated first before any measurement, cyclic voltametry (CV) measurements were thus executed under various scan rates in the presence of 1mM glucose in 500mM NaOH solution, ranging from 25 to 200mV/s. As shown in **Figure 17**. (a), both anodic and cathodic peak currents increase in parallel with the potential scan rate, and a linear relationship between peak current and the square root of the scan rate was

found in **Figure. 17** (b), which indicated a diffusion-controlled process (Yoon et al., 2011; Zhang et al., 2016).

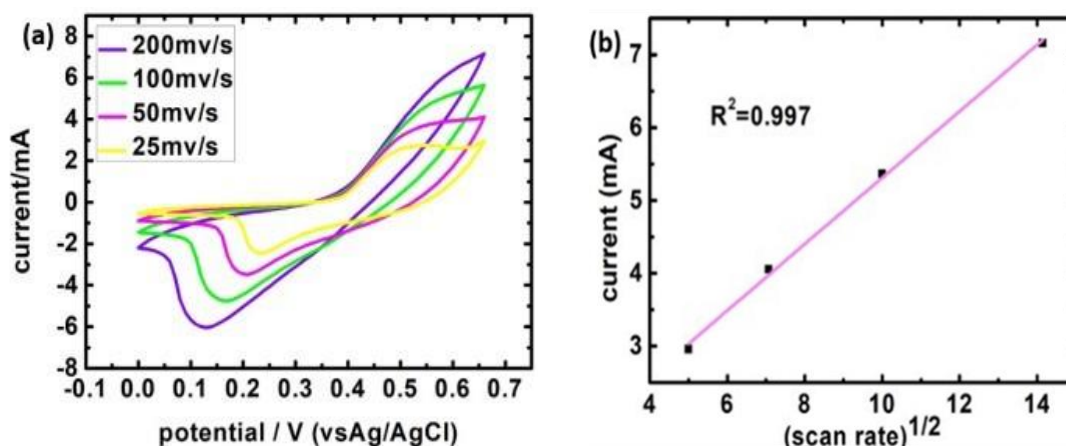


Figure. 17 (a) CV responses of Ni(OH)₂/NiOOH electrode in the presence of 1mM glucose in 500mM NaOH solution under various scan rates; (b) the relationship between the current and scan rate.

3.2.4 Amperometric investigations

Systematic investigations have been followed by amperometric measurements in electrolytes of various OH⁻ concentrations, leading to the finding that the maximum value of glucose concentration in the linear range was 1/25 of the OH⁻ concentration, which has never been reported. In **Figure 18** a–c, a typical amperometric response of the Ni (OH)₂/Ni sheet upon the successive addition of a certain concentration of glucose into 0.1 mM, 500 mM and 1000 mM NaOH solution stirred at 350 rpm is shown. These three amperometric I-t step curves were used to calculate the linear range of glucose sensing in 500mM, 100mM and 1000mM NaOH solutions, respectively.

Figure. 18d–f shows the calibration curve of the $\text{Ni}(\text{OH})_2/\text{Ni}$ sheet electrode, revealing a good linear detection ranging from $21.67 \mu\text{M}$ to 4 mM ($R_2 = 0.9905$) in 100 mM NaOH solution, from $7.40 \mu\text{M}$ to 20 mM ($R_2 = 0.9955$) in 500 mM NaOH solution, and from $39.98 \mu\text{M}$ to 40 mM ($R_2 = 0.9949$) in 1000 mM NaOH solution. By a signal-to-noise ratio of 3, the detection limits (LOD) were estimated to be $7.15 \mu\text{M}$, $2.44 \mu\text{M}$, and $13.19 \mu\text{M}$, respectively. Besides, it was found that the linear range was successfully increased to 40 mM in 1000 mM NaOH solution. More importantly, **Figure. 18 d–f** shows the ratio of the highest point of the linear range and OH^- concentration was fixed at around 25, which meant the linear range could be enhanced by raising the OH^- concentration.

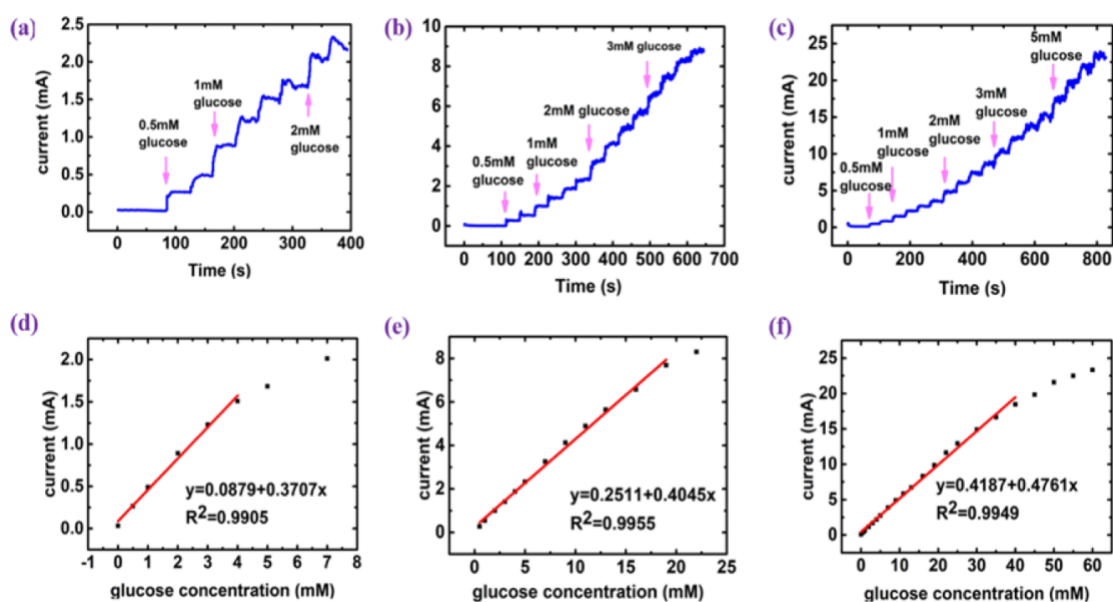


Figure. 18 (a) The amperometric I-t curve at $[\text{OH}^-] = 100 \text{ mM}$; (b) the amperometric I-t curve at $[\text{OH}^-] = 500 \text{ mM}$; (c) the amperometric I-t curve at $[\text{OH}^-] = 1000 \text{ mM}$; (d) the calibration curve at $[\text{OH}^-] = 100 \text{ mM}$; (e) the calibration curve at $[\text{OH}^-] = 500 \text{ mM}$; (f) the calibration curve at $[\text{OH}^-] = 1000 \text{ mM}$.

[OH⁻] = 500 mM; the linear range concentration of glucose at various OH⁻ concentrations, (d) [OH⁻] = 100 mM, (e) [OH⁻] = 500 mM and (f) [OH⁻] = 1000 mM.

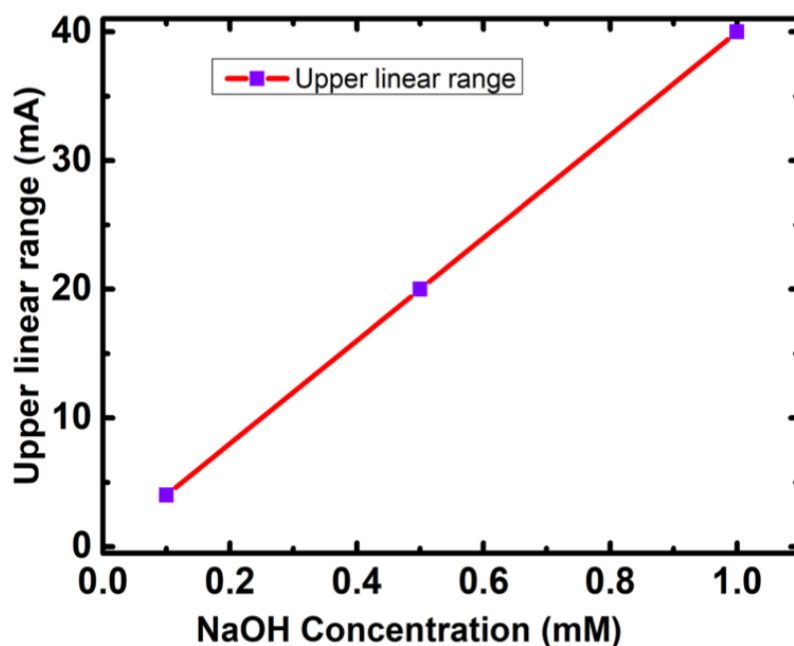


Figure. 19 The relationship between electrolyte solution concentration and upper linear range of detection glucose

In fact, our findings can be further confirmed by the literature results, which also show a definite ratio between the hydroxide ion concentration and the linear range, but so far surprisingly ignored (Cooray et al., 2017; Kang et al., 2007; Ma et al., 2017; Niu et al., 2013; Wu et al., 2016; Zhang et al., 2015). As presented in **Table 1**, measurements of the glucose level were conducted at 100mM NaOH or KOH

solution in many other non-enzymatic glucose sensors, whose linear ranges were mostly hovered at 4mM. Based on our findings on linear scales, these efforts have been confirmed. This means that in other types of sensors, the relationship between glucose concentration and alkaline concentration is also maintained.

Table 1. The relationship between the linear range and the alkaline level of various non-enzymatic glucose sensors.

Other non-enzymatic glucose sensors	[OH]⁻ (mM)	Linear range (mM)	Ratio of [OH]⁻ / Linear range	Sensitivity (mA/mM cm²)	LOD (μM)
Cu-CNTs-GCE (Kang et al., 2009)	100	Up to 3.5	28.5	0.01776	0.2
3D porous Ni/SPCE (Niu et al., 2013)	100	Up to 4	25	2.9	0.07

Ni₆S₇/GCE (Wu et al., 2016)	100	Up to 3.75	26.7	0.2718	0.15
CuO/GCE (Ma et al., 2017)	100	Up to 4	25	1.322	0.5
Fe₃O₄/Fe foil (Zhang et al., 2015)	100	Up to 3.67	27.2	0.407	0.1
CoSe-rGO/GCE (Cooray et al., 2017)	300	Up to 10	30	0.48	2.5
Ni(OH)₂/NiOOH foil (our results)	1000	Up to 40	25	2.645	13.19

CNTs (carbon nanotubes); GCE (glassy carbon electrode); SPCE (screen-printed carbon electrode); rGO (reduced graphene oxide).

3.2.5 Anti-interference ability

The anti-interference test of the Ni(OH)₂/Ni sheet electrode was further evaluated. Since in biological samples such as blood, in addition to glucose, there are other substances that are easily oxidized, such as lactic acid (LA), ascorbic acid (AA), urea, sodium citrate, galactose, fructose, sodium benzoate and L-cysteine. The designed platform should have acceptable selectivity for glucose compared to the coexistence of interfering species (Promsuwan et al., 2019). The physiological level of normal glucose concentration is in the range of 3-8mM, which is much higher than the concentration level of interfering substances like AA (0.1 mM), L-cysteine (15μM), etc. (Park et al., 2003). **Figure. 20 (a)** depicts an amperometry graph of 1 mM glucose after adding 1 mM LA, AA, urea, sodium citrate, galactose, fructose, sodium benzoate and L-cysteine to a 0.1 M NaOH stirring solution at +0.5 V (vs. Ag / AgCl) potentials, respectively. The histogram of **Figure. 20(b)** compares the current response of glucose detection with other interfering substances. As can be seen from the figure, the responses caused by interfering species are very low, for example, for 1 mM LA (~ 5.04%), 1 mM AA (~ 12.3%), 1 mM urea (~ 6.9%), 1 mM sodium citrate (~ 0.18%), 1 mM galactose (~ 6.8%), 1 mM fructose (~ 4.4%), 1 mM sodium benzoate (~ 0.35%) and 1 mM L-cysteine (~ 0.3%). These results indicate that interfering substances slightly interfere with the oxidation of glucose, but these small current changes are negligible compared to the current generated by the addition of 1 mM glucose. The results show that our modified electrode can be used as a selective non-enzymatic sensing platform for glucose detection.

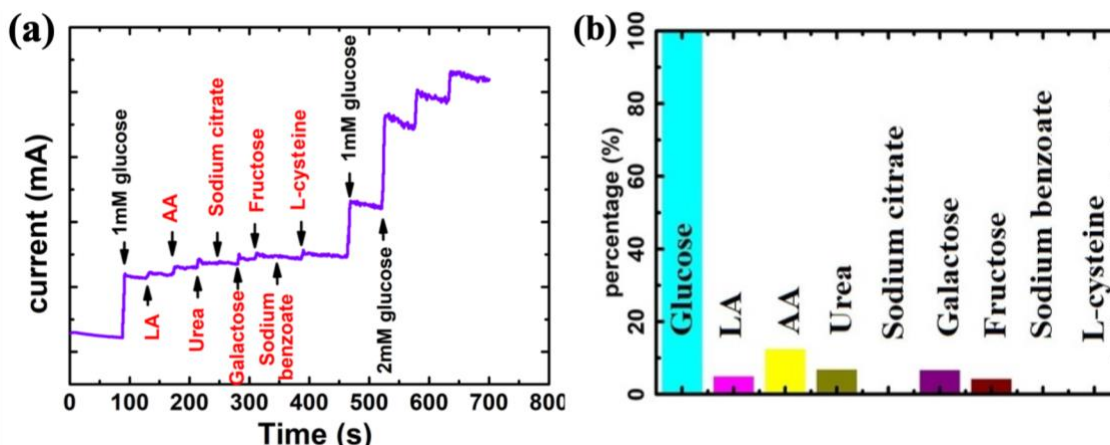


Figure. 20 (a) Current responses of the Ni(OH)₂/Ni sheet electrode after adding 1 mM glucose following by the injection of 1 mM LA, AA, urea, sodium citrate, galactose, fructose, sodium benzoate and L-cysteine with 35 s intervals into stirring 1 M NaOH solution at the constant potential of +0.5 V (vs. Ag/AgCl), respectively, (b) Column chart for the comparison between the response of the electrode toward 1 mM glucose against 0.1 mM LA, AA, urea, sodium citrate, galactose, fructose, sodium benzoate and L-cysteine.

3.3 FTIR test

Clearly, OH⁻ affected the glucose electro-oxidation reaction, which needed further investigation by FTIR measurements. The pure glucose electro-oxidized product, glucose/NaOH mixture, and glucose/NaOH electro-oxidized mixture were measured by FTIR. As shown in **Figure 21** a, the peak of the C=C double bond was detected in the glucose/NaOH mixture at 1670 cm⁻¹ (Lin et al., 2007),

which indicated the formation of enediol(Larew and Johnson, 1989). This means glucose reacted with NaOH before the electro-oxidation. In addition, the disappearance of the peak at 1080 cm^{-1} and 1350 cm^{-1} in glucose/NaOH electro-oxidized mixture in **Figure 21 b** proved that the electro-oxidation product was not gluconate, which indicated that more than four electrons were transferred to the cathode(Bae et al., 1991; Chang et al., 1991; Holade et al., 2018; Sugars and Alkaline, 1969). This was beneficial for glucose sensing.

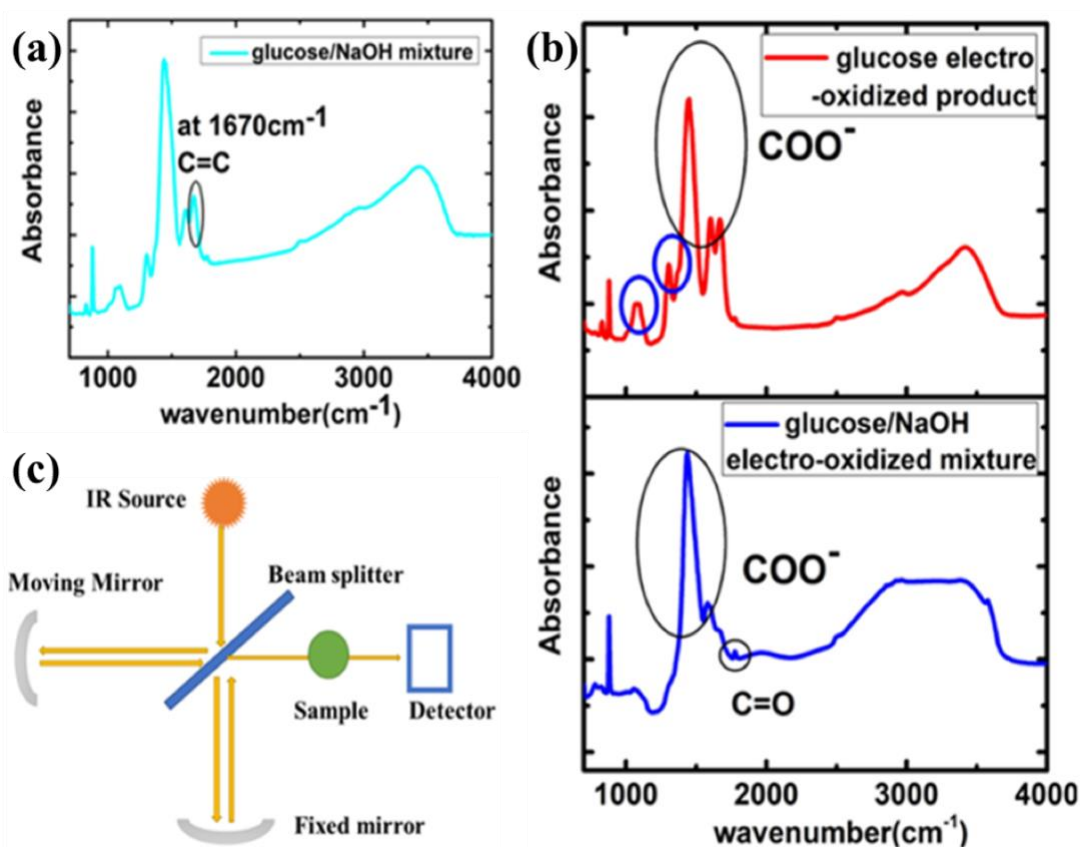


Figure. 21 (a) Fourier-transform infrared spectroscopy (FTIR) results of glucose/NaOH mixture; (b) FTIR results of a pure glucose electro-oxidized product and glucose/NaOH electro-oxidized mixture were measured by FTIR.

3.4 UV and NMR test

Further evidence was obtained by the UV and NMR measurements. As shown in **Figure. 22**, a new absorption peak was observed in glucose/NaOH mixture solution at 278 nm, which was attributed to enediol(Chen et al., 2012; Zhao et al., 2011). Similar results could also be found in NMR data, as shown in **Figure. 23**, where two $-CH_2$ groups were detected, indicating the transformation of glucose to enediol.

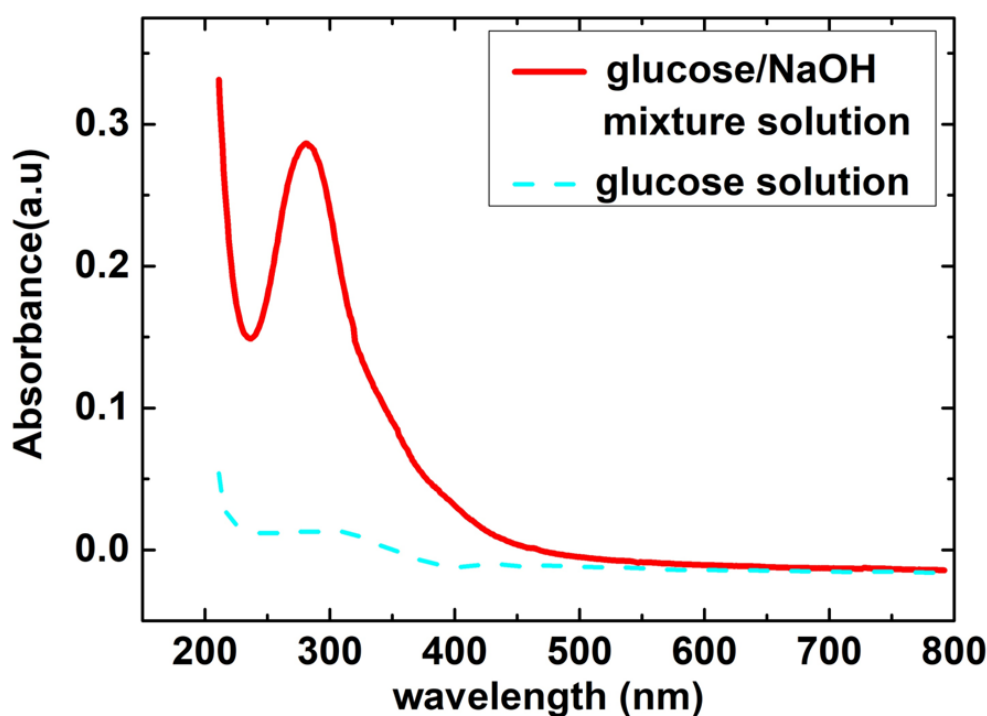


Figure. 22 UV-vis spectra of the glucose/NaOH mixture solution (solid line) and glucose solution (dash line).

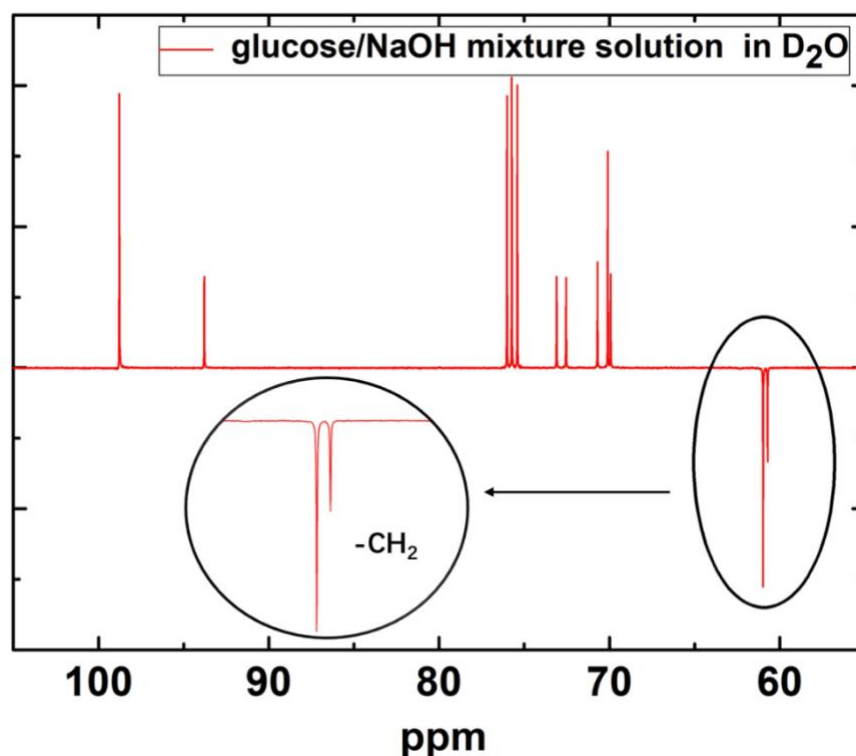


Figure. 23 ^{13}C DEPTQ-135 NMR spectrum of glucose/NaOH mixture dissolved in D_2O with a frequency of 125.78 MHz.

It is clear now that we discovered the reason behind the limited linear range and enhanced successfully such a range to 40 mM, which was in sharp contrast to the literature, where the linear range was limited, and the reason was neglected (Annalakshmi et al., 2019; Park et al., 2003; Pradhan et al., 2010; Rong et al., 2007). Although a similar relationship between the linear range and OH^- concentration can also be extracted in other literature, this relationship was overlooked before. The actual influence of hydroxide ions was found to be on the reaction with glucose. When the OH^- concentration is low, the glucose electro-oxidation reaction only transfers two electrons to the cathode, as opposed to the four or more electrons transferred in the electrolyte with high OH^- concentration. Subsequently, the current response was reduced, which corresponded to the non-linear range in the I-t curve. Therefore, insufficient

OH⁻ concentration in the electrolyte was the real cause that limited the linear range, instead of the electrode passivation or limited electrode potential(Annalakshmi et al., 2019).

To summarize, high OH⁻ concentration is beneficial for glucose sensing, glucose could react with hydroxide ions, generating enediol, which lowered the energy barrier of the electro-oxidation reaction and more than four electrons are transferred to the cathode(Larew and Johnson, 1989). The final product was glucuronate (Equation (2)), instead of gluconolactone (Equation (3)). More than four electrons were transferred in this case, indicating a higher measured current in the I-t curve, which could not only increase the linear range but also the measurement accuracy.



4 Conclusion

In conclusion, the root cause of the limited linear range of glucose sensor has been successfully revealed, which is attributed to the alkaline concentration (hydroxide ion concentration), affecting the degree and final product of glucose oxidation. By increasing the concentration of hydroxide ions, not only the linear range is increased up to 40 mM, but also the conversion rate of NiOOH / Ni(OH)₂ is increased, which can also improve the sensitivity of the glucose sensor, indicating better measurement accuracy. These findings are expected to have some impact on the non-enzymatic glucose monitoring community, as they may open new avenues for biomedical sensing.

5 Reference

- Alwarappan, S., Erdem, A., Liu, C., Li, C.Z., 2009. Probing the electrochemical properties of graphene nanosheets for biosensing applications. *J. Phys. Chem. C*. <https://doi.org/10.1021/jp9010313>
- Annalakshmi, M., Balasubramanian, P., Chen, S.M., Chen, T.W., 2019. Enzyme-free electrocatalytic sensing of hydrogen peroxide using a glassy carbon electrode modified with cobalt nanoparticle-decorated tungsten carbide. *Microchim. Acta*. <https://doi.org/10.1007/s00604-019-3377-x>
- Armour, J.C., Lucisano, J.Y., McKean, B.D., Gough, D.A., 1990. Application of chronic intravascular blood glucose sensor in dogs. *Diabetes*. <https://doi.org/10.2337/diab.39.12.1519>
- Bae, I.T., Yeager, E., Xing, X., Liu, C.C., 1991. In situ infrared studies of glucose oxidation on platinum in an alkaline medium. *J. Electroanal. Chem.* 309, 131–145. [https://doi.org/10.1016/0022-0728\(91\)87009-S](https://doi.org/10.1016/0022-0728(91)87009-S)
- Bernards, D.A., MacAya, D.J., Nikolou, M., Defranco, J.A., Takamatsu, S., Malliaras, G.G., 2008. Enzymatic sensing with organic electrochemical transistors. *J. Mater. Chem.* <https://doi.org/10.1039/b713122d>
- Besteman, K., Lee, J.O., Wiertz, F.G.M., Heering, H.A., Dekker, C., 2003. Enzyme-coated carbon nanotubes as single-molecule biosensors. *Nano Lett.* <https://doi.org/10.1021/nl034139u>

- Brauker, J., 2009. Continuous glucose sensing: Future technology developments. *Diabetes Technol. Ther.* <https://doi.org/10.1089/dia.2008.0137>
- Bruen, D., Delaney, C., Florea, L., Diamond, D., 2017. Glucose sensing for diabetes monitoring: Recent developments. *Sensors (Switzerland)*. <https://doi.org/10.3390/s17081866>
- Cha, K.H., Meyerhoff, M.E., 2017. Compatibility of Nitric Oxide Release with Implantable Enzymatic Glucose Sensors Based on Osmium (III/II) Mediated Electrochemistry. *ACS Sensors*. <https://doi.org/10.1021/acssensors.7b00430>
- Chang, S.C., Ho, Y., Weaver, M.J., 1991. Applications of Real-Time FTIR Spectroscopy to the Elucidation of Complex Electroorganic Pathways: Electrooxidation of Ethylene Glycol on Gold, Platinum, and Nickel in Alkaline Solution. *J. Am. Chem. Soc.* 113, 9506–9513. <https://doi.org/10.1021/ja00025a014>
- Chase, H.P., Beck, R.W., Xing, D., Tamborlane, W. V., Coffey, J., Fox, L.A., Ives, B., Keady, J., Kollman, C., Laffel, L., Ruedy, K.J., 2010. Continuous glucose monitoring in youth with type 1 diabetes: 12-month follow-up of the juvenile diabetes research foundation continuous glucose monitoring randomized trial. *Diabetes Technol. Ther.* <https://doi.org/10.1089/dia.2010.0021>

- Chaubey, A., Malhotra, B.D., 2002. Mediated biosensors. *Biosens. Bioelectron.*
[https://doi.org/10.1016/S0956-5663\(01\)00313-X](https://doi.org/10.1016/S0956-5663(01)00313-X)
- Chen, C., Xie, Q., Yang, D., Xiao, H., Fu, Y., Tan, Y., Yao, S., 2013. Recent advances in electrochemical glucose biosensors: A review. *RSC Adv.*
<https://doi.org/10.1039/c2ra22351a>
- Chen, J., Zhao, C.X., Zhi, M.M., Wang, K., Deng, L., Xu, G., 2012. *Electrochimica Acta* Alkaline direct oxidation glucose fuel cell system using silver / nickel foams as electrodes 66, 133–138.
<https://doi.org/10.1016/j.electacta.2012.01.071>
- Chen, J.Y., Zhou, Q., Xu, G., Wang, R.T., Tai, E.G., Xie, L., Zhang, Q., Guan, Y., Huang, X., 2019. Non-invasive blood glucose measurement of 95% certainty by pressure regulated Mid-IR. *Talanta.*
<https://doi.org/10.1016/j.talanta.2019.01.034>
- Chen, Xiaomei, Wu, G., Cai, Z., Oyama, M., Chen, Xi, 2014. Advances in enzyme-free electrochemical sensors for hydrogen peroxide, glucose, and uric acid. *Microchim. Acta.* <https://doi.org/10.1007/s00604-013-1098-0>
- Cherevko, S., Chung, C.H., 2009. Gold nanowire array electrode for non-enzymatic voltammetric and amperometric glucose detection. *Sensors Actuators, B Chem.* <https://doi.org/10.1016/j.snb.2009.07.023>

- Chinnadayala, S.R., Park, K.D., Cho, S., 2018. Editors' Choice—Review—In Vivo and In Vitro Microneedle Based Enzymatic and Non-Enzymatic Continuous Glucose Monitoring Biosensors. *ECS J. Solid State Sci. Technol.* <https://doi.org/10.1149/2.0241807jss>
- Cho, N.H., Shaw, J.E., Karuranga, S., Huang, Y., da Rocha Fernandes, J.D., Ohlogge, A.W., Malanda, B., 2018. IDF Diabetes Atlas: Global estimates of diabetes prevalence for 2017 and projections for 2045. *Diabetes Res. Clin. Pract.* <https://doi.org/10.1016/j.diabres.2018.02.023>
- Cooray, M.C.D., Zhang, X., Zhang, Y., Langford, S.J., Bond, A.M., Zhang, J., 2017. Cobalt selenide nanoflake decorated reduced graphene oxide nanocomposite for efficient glucose electro-oxidation in alkaline medium. *J. Mater. Chem. A.* <https://doi.org/10.1039/c7ta04742h>
- Cui, G., Yoo, J.H., Woo, B.W., Kim, S.S., Cha, G.S., Nam, H., 2001. Disposable amperometric glucose sensor electrode with enzyme-immobilized nitrocellulose strip. *Talanta.* [https://doi.org/10.1016/S0039-9140\(01\)00377-0](https://doi.org/10.1016/S0039-9140(01)00377-0)
- da Rocha Fernandes, J., Ogurtsova, K., Linnenkamp, U., Guariguata, L., Seuring, T., Zhang, P., Cavan, D., Makaroff, L.E., 2016. IDF Diabetes Atlas estimates of 2014 global health expenditures on diabetes. *Diabetes Res. Clin. Pract.* <https://doi.org/10.1016/j.diabres.2016.04.016>

- De Poulpiquet, A., Ciaccafava, A., Lojou, E., 2014. New trends in enzyme immobilization at nanostructured interfaces for efficient electrocatalysis in biofuel cells. *Electrochim. Acta*.
<https://doi.org/10.1016/j.electacta.2013.07.133>
- Ding, Y., Liu, Y., Zhang, L., Wang, Y., Bellagamba, M., Parisi, J., Li, C.M., Lei, Y., 2011. Sensitive and selective nonenzymatic glucose detection using functional NiO-Pt hybrid nanofibers. *Electrochim. Acta*.
<https://doi.org/10.1016/j.electacta.2011.09.039>
- Dong, Q., Song, D., Huang, Y., Xu, Z., Chapman, J.H., Willis, W.S., Li, B., Lei, Y., 2018. High-temperature annealing enabled iridium oxide nanofibers for both non-enzymatic glucose and solid-state pH sensing. *Electrochim. Acta*.
<https://doi.org/10.1016/j.electacta.2018.04.205>
- Editor, S., n.d. 2008_Book_BiosensingForThe21stCentury.
- Elgrishi, N., Rountree, K.J., McCarthy, B.D., Rountree, E.S., Eisenhart, T.T., Dempsey, J.L., 2018. A Practical Beginner's Guide to Cyclic Voltammetry. *J. Chem. Educ.* <https://doi.org/10.1021/acs.jchemed.7b00361>
- Fajardo, S., García-Galvan, R., F., Barranco, V., Galvan, J.C., Batlle, S.F., 2016. We are IntechOpen , the world ' s leading publisher of Open Access books Built by scientists , for scientists TOP 1 % . Intech i, 13.
<https://doi.org/http://dx.doi.org/10.5772/57353>

Freire, R.S., Pessoa, C.A., Mello, L.D., Kubota, L.T., 2003. Direct electron transfer: An approach for electrochemical biosensors with higher selectivity and sensitivity. *J. Braz. Chem. Soc.* <https://doi.org/10.1590/S0103-50532003000200008>

Gonzales, W.V., Mobashsher, A.T., Abbosh, A., 2019. The progress of glucose monitoring—A review of invasive to minimally and non-invasive techniques, devices and sensors, *Sensors (Switzerland)*. <https://doi.org/10.3390/s19040800>

Gorton, L., Bremle, G., Csöregi, E., Jönsson-Pettersson, G., Persson, B., 1991. Amperometric glucose sensors based on immobilized glucose-oxidizing enzymes and chemically modified electrodes. *Anal. Chim. Acta.* [https://doi.org/10.1016/0003-2670\(91\)87006-S](https://doi.org/10.1016/0003-2670(91)87006-S)

Gupta, V.K., Atar, N., Yola, M.L., Eryilmaz, M., Torul, H., Tamer, U., Boyaci, I.H., Üstündağ, Z., 2013. A novel glucose biosensor platform based on Ag@AuNPs modified graphene oxide nanocomposite and SERS application. *J. Colloid Interface Sci.* <https://doi.org/10.1016/j.jcis.2013.06.007>

Habermüller, K., Mosbach, M., Schuhmann, W., 2000. Electron-transfer mechanisms in amperometric biosensors. *Fresenius. J. Anal. Chem.* <https://doi.org/10.1007/s002160051551>

- Harper, A., Anderson, M.R., 2010. Electrochemical glucose sensors- developments using electrostatic assembly and carbon nanotubes for biosensor construction. *Sensors*. <https://doi.org/10.3390/s100908248>
- Holade, Y., Engel, A.B., Servat, K., Napporn, T.W., Morais, C., Tingry, S., Cornu, D., Boniface Kokoh, K., 2018. Electrocatalytic and electroanalytic investigation of carbohydrates oxidation on gold-based nanocatalysts in alkaline and neutral pHs. *J. Electrochem. Soc.* 165, H425–H436. <https://doi.org/10.1149/2.0311809jes>
- Hwang, D.W., Lee, S., Seo, M., Chung, T.D., 2018. Recent advances in electrochemical non-enzymatic glucose sensors – A review. *Anal. Chim. Acta*. <https://doi.org/10.1016/j.aca.2018.05.051>
- International Diabetes Federation., 2017. *IDF Diabetes Atlas, IDF Diabetes Atlas, 8th edition*. [https://doi.org/http://dx.doi.org/10.1016/S0140-6736\(16\)31679-8](https://doi.org/http://dx.doi.org/10.1016/S0140-6736(16)31679-8).
- Jia, L., Wei, X., Lv, L., Zhang, X., Duan, X., Xu, Y., Liu, K., Wang, J., 2018. Electrodeposition of hydroxyapatite on nickel foam and further modification with conductive polyaniline for non-enzymatic glucose sensing. *Electrochim. Acta*. <https://doi.org/10.1016/j.electacta.2018.05.130>
- Kang, X., Mai, Z., Zou, X., Cai, P., Mo, J., 2007. A sensitive nonenzymatic glucose sensor in alkaline media with a copper nanocluster/multiwall

carbon nanotube-modified glassy carbon electrode. *Anal. Biochem.*

<https://doi.org/10.1016/j.ab.2007.01.003>

Kang, X., Wang, J., Wu, H., Aksay, I.A., Liu, J., Lin, Y., 2009. Glucose Oxidase-graphene-chitosan modified electrode for direct electrochemistry and glucose sensing. *Biosens. Bioelectron.*

<https://doi.org/10.1016/j.bios.2009.09.004>

Karunakaran, C., Madasamy, T., Sethy, N.K., 2015. Enzymatic Biosensors, in: *Biosensors and Bioelectronics*. <https://doi.org/10.1016/B978-0-12-803100-1.00003-7>

Kashyap, S., Lu, F., 1998. Oxygen-rich oxidase enzyme electrodes for operation in oxygen-free solutions. *J. Am. Chem. Soc.*

<https://doi.org/10.1021/ja972759p>

Kim, S., Kim, K., Kim, H.J., Lee, H.N., Park, T.J., Park, Y.M., 2018. Non-enzymatic electrochemical lactate sensing by NiO and Ni(OH)₂ electrodes: A mechanistic investigation. *Electrochim. Acta.*

<https://doi.org/10.1016/j.electacta.2018.04.172>

Larew, L.A., Johnson, D.C., 1989. Concentration dependence of the mechanism of glucose oxidation at gold electrodes in alkaline media 262, 167–182.

Léger, C., Elliott, S.J., Hoke, K.R., Jeuken, L.J.C., Jones, A.K., Armstrong, F.A., 2003. Enzyme electrokinetics: Using protein film voltammetry to

investigate redox enzymes and their mechanisms. *Biochemistry*.

<https://doi.org/10.1021/bi034789c>

Li, M., Bo, X., Mu, Z., Zhang, Y., Guo, L., 2014. Electrodeposition of nickel oxide and platinum nanoparticles on electrochemically reduced graphene oxide film as a nonenzymatic glucose sensor. *Sensors Actuators, B Chem.* 192, 261–268. <https://doi.org/10.1016/j.snb.2013.10.140>

Li, X., Yao, J., Liu, F., He, H., Zhou, M., Mao, N., Xiao, P., Zhang, Y., 2013. Nickel/Copper nanoparticles modified TiO₂ nanotubes for non-enzymatic glucose biosensors. *Sensors Actuators, B Chem.* <https://doi.org/10.1016/j.snb.2013.02.035>

Liberman, A., Buckingham, B., Phillip, M., 2011. Diabetes technology and the human factor. *Int. J. Clin. Pract. Suppl.* <https://doi.org/10.1111/j.1742-1241.2010.02583.x>

Lin, S., Li, M., Cheng, W., 2007. FT-IR and Raman vibrational microspectroscopies used for spectral biodiagnosis of human tissues 21, 1–30.

Liu, C.C., 2006. Electrochemical sensors, in: *Medical Devices and Systems*. <https://doi.org/10.5796/kogyobutsurikagaku.58.1087>

- Liu, J., Agarwal, M., Varahramyan, K., 2008. Glucose sensor based on organic thin film transistor using glucose oxidase and conducting polymer. *Sensors Actuators, B Chem.* <https://doi.org/10.1016/j.snb.2008.08.009>
- Liu, J., Chou, A., Rahmat, W., Paddon-Row, M.N., Gooding, J.J., 2005. Achieving direct electrical connection to glucose oxidase using aligned single walled carbon nanotube arrays. *Electroanalysis* 17, 38–46. <https://doi.org/10.1002/elan.200403116>
- Liu, S., Liu, B., Gong, C., Li, Z., 2019. A nanoporous Cu-Ag thin film at the Cu-Ag-Zn alloy surface by spontaneous dissolution of Zn and Cu in different degrees as a highly sensitive non-enzymatic glucose sensor. *Electrochim. Acta.* <https://doi.org/10.1016/j.electacta.2019.134599>
- Luo, J., Jiang, S., Zhang, H., Jiang, J., Liu, X., 2012. A novel non-enzymatic glucose sensor based on Cu nanoparticle modified graphene sheets electrode. *Anal. Chim. Acta.* <https://doi.org/10.1016/j.aca.2011.10.025>
- Ma, X., Zhao, Q., Wang, H., Ji, S., 2017. Controlled synthesis of CuO from needle to flower-like particle morphologies for highly sensitive glucose detection. *Int. J. Electrochem. Sci.* <https://doi.org/10.20964/2017.09.37>
- Mahshid, S.S., Mahshid, S., Dolati, A., Ghorbani, M., Yang, L., Luo, S., Cai, Q., 2013. Electrodeposition and electrocatalytic properties of Pt/Ni-Co nanowires for non-enzymatic glucose detection. *J. Alloys Compd.* 554, 169–176. <https://doi.org/10.1016/j.jallcom.2012.10.186>

Malitesta, C., Palmisano, F., Torsi, L., Zambonin, P.G., 1990. Glucose Fast-Response Amperometric Sensor Based on Glucose Oxidase Immobilized in an Electropolymerized Poly(o-phenylenediamine) Film. *Anal. Chem.*
<https://doi.org/10.1021/ac00223a016>

Martins, M.V.A., Pereira, A.R., Luz, R.A.S., Iost, R.M., Crespilho, F.N., 2014. Evidence of short-range electron transfer of a redox enzyme on graphene oxide electrodes. *Phys. Chem. Chem. Phys.*
<https://doi.org/10.1039/c4cp00452c>

Nagata, R., Yokoyama, K., Clark, S.A., Karube, I., 1995. A glucose sensor fabricated by the screen printing technique. *Biosens. Bioelectron.*
[https://doi.org/10.1016/0956-5663\(95\)96845-P](https://doi.org/10.1016/0956-5663(95)96845-P)

Newcomer, J.W., 2005. Second-generation (atypical) antipsychotics and metabolic effects: A comprehensive literature review. *CNS Drugs.*
<https://doi.org/10.2165/00023210-200519010-00001>

Niu, X., Lan, M., Zhao, H., Chen, C., 2013. Highly sensitive and selective nonenzymatic detection of glucose using three-dimensional porous nickel nanostructures. *Anal. Chem.* <https://doi.org/10.1021/ac3030976>

Niu, X., Li, X., Pan, J., He, Y., Qiu, F., Yan, Y., 2016. Recent advances in non-enzymatic electrochemical glucose sensors based on non-precious transition metal materials: Opportunities and challenges. *RSC Adv.*
<https://doi.org/10.1039/c6ra12506a>

- O'Connell, P.J., Hawthorne, W.J., Holmes-Walker, D.J., Nankivell, B.J., Gunton, J.E., Patel, A.T., Walters, S.N., Pleass, H.C.C., Allen, R.D.M., Chapman, J.R., 2006. Clinical islet transplantation in type 1 diabetes mellitus: Results of Australia's first trial. *Med. J. Aust.*
<https://doi.org/10.5694/j.1326-5377.2006.tb00206.x>
- Oliver, N.S., Toumazou, C., Cass, A.E.G., Johnston, D.G., 2009. Glucose sensors: A review of current and emerging technology. *Diabet. Med.*
<https://doi.org/10.1111/j.1464-5491.2008.02642.x>
- Park, S., Boo, H., Chung, T.D., 2006. Electrochemical non-enzymatic glucose sensors. *Anal. Chim. Acta.* <https://doi.org/10.1016/j.aca.2005.05.080>
- Park, S., Chung, T.D., Kim, H.C., 2003. Nonenzymatic Glucose Detection Using Mesoporous Platinum 75, 3046–3049. <https://doi.org/10.1021/ac0263465>
- Pradhan, D., Niroui, F., Leung, K.T., 2010. High-performance, flexible enzymatic glucose biosensor based on ZnO nanowires supported on a gold-coated polyester substrate. *ACS Appl. Mater. Interfaces.*
<https://doi.org/10.1021/am100413u>
- Promsuwan, K., Kachatong, N., Limbut, W., 2019. Electrochimica Acta Simple flow injection system for non-enzymatic glucose sensing based on an electrode modified with palladium nanoparticles- graphene nanoplatelets / multi-walled carbon nanotubes. *Electrochim. Acta* 320, 134621.
<https://doi.org/10.1016/j.electacta.2019.134621>

- Pumera, M., Sánchez, S., Ichinose, I., Tang, J., 2007. Electrochemical nanobiosensors. *Sensors Actuators, B Chem.*
<https://doi.org/10.1016/j.snb.2006.11.016>
- Putzbach, W., Ronkainen, N.J., 2013. Immobilization techniques in the fabrication of nanomaterial-based electrochemical biosensors: A review. *Sensors (Switzerland)*. <https://doi.org/10.3390/s130404811>
- Raveendran, J., Resmi, P.E., Ramachandran, T., Nair, B.G., Satheesh Babu, T.G., 2017. Fabrication of a disposable non-enzymatic electrochemical creatinine sensor. *Sensors Actuators, B Chem.*
<https://doi.org/10.1016/j.snb.2016.11.158>
- Renard, E., 2005. Monitoring glycemic control: The importance of self-monitoring of blood glucose. *Am. J. Med.*
<https://doi.org/10.1016/j.amjmed.2005.07.052>
- Risérus, U., Willett, W.C., Hu, F.B., 2009. Dietary fats and prevention of type 2 diabetes. *Prog. Lipid Res.* <https://doi.org/10.1016/j.plipres.2008.10.002>
- Rolland, F., Baena-Gonzalez, E., Sheen, J., 2006. SUGAR SENSING AND SIGNALING IN PLANTS: Conserved and Novel Mechanisms. *Annu. Rev. Plant Biol.* <https://doi.org/10.1146/annurev.arplant.57.032905.105441>

- Rong, L.Q., Yang, C., Qian, Q.Y., Xia, X.H., 2007. Study of the nonenzymatic glucose sensor based on highly dispersed Pt nanoparticles supported on carbon nanotubes. *Talanta*. <https://doi.org/10.1016/j.talanta.2006.12.037>
- Scheller, F.W., Schubert, F., Neumann, B., Pfeiffer, D., Hintsche, R., Dransfeld, I., Wollenberger, U., Renneberg, R., Warsinke, A., Johansson, G., Skoog, M., Yang, X., Bogdanovskaya, V., Bückmann, A., Zaitsev, S.Y., 1991. Second generation biosensors. *Biosens. Bioelectron.* [https://doi.org/10.1016/0956-5663\(91\)80010-U](https://doi.org/10.1016/0956-5663(91)80010-U)
- Shadlaghani, A., Farzaneh, M., Kinser, D., Reid, R.C., 2019. Direct electrochemical detection of glutamate, acetylcholine, choline, and adenosine using non-enzymatic electrodes. *Sensors (Switzerland)*. <https://doi.org/10.3390/s19030447>
- Shim, N.Y., Bernardis, D.A., Macaya, D.J., DeFranco, J.A., Nikolou, M., Owens, R.M., Malliaras, G.G., 2009. All-plastic electrochemical transistor for glucose sensing using a ferrocene mediator. *Sensors*. <https://doi.org/10.3390/s91209896>
- Song, M.J., Hwang, S.W., Whang, D., 2010. Non-enzymatic electrochemical CuO nanoflowers sensor for hydrogen peroxide detection. *Talanta*. <https://doi.org/10.1016/j.talanta.2009.09.061>

Spanning, A., Neujahr, H.Y., 1990. The effect of glucose on enzyme activities and phenol utilization in *Trichosporon cutaneum* grown in continuous culture. *J. Gen. Microbiol.* <https://doi.org/10.1099/00221287-136-8-1491>

Sugars, O.F., Alkaline, I.N., 1969. 163 transformations 9.

Tamborlane, W. V., Beck, R.W., Bode, B.W., Buckingham, B., Chase, H.P., Clemons, R., Fiallo-Scharer, R., Fox, L.A., Gilliam, L.K., Hirsch, I.B., Huang, E.S., Kollman, C., Kowalski, A.J., Laffel, L., Lawrence, J.M., Lee, J., Mauras, N., O'Grady, M., Ruedy, K.J., Tansey, M., Tsalikian, E., Weinzimer, S., Wilson, D.M., Wolpert, H., Wysocki, T., Xing, D., Messer, L., Gage, V., Burdick, P., Milaszewski, K., Pratt, K., Bismuth, E., Keady, J., Lawlor, M., Block, J., Benassi, K., Kucera, D., Coffey, J., Cabbage, J., Shetty, G., Atakov-Castillo, A., Giusti, J., O'Donnell, S., Ghiloni, S., Fitzpatrick, K., Khakpour, D., Englert, K., Permuy, J., O'Neil, K., Tolbert, L., Maeva, M., Sattler, B., Ives, B., Bosson-Heenan, J., Jackson, J., Steffes, M., Bucksa, J.M., Nowicki, M.L., Van Hale, C., Makky, V., Basu, A., Meltzer, D.O., Zhao, L., Weinstock, R.S., Anderson, B.J., Kruger, D., LaVange, L., Rodriguez, H., 2008. Continuous glucose monitoring and intensive treatment of type 1 diabetes. *N. Engl. J. Med.* <https://doi.org/10.1056/NEJMoa0805017>

Toghill, K.E., Compton, R.G., 2010. Electrochemical non-enzymatic glucose sensors: A perspective and an evaluation. *Int. J. Electrochem. Sci.*

- Tremey, E., Suraniti, E., Courjean, O., Gounel, S., Stines-Chaumeil, C., Louerat, F., Mano, N., 2014. Switching an O₂ sensitive glucose oxidase bioelectrode into an almost insensitive one by cofactor redesign. *Chem. Commun.* 50, 5912–5914. <https://doi.org/10.1039/c4cc01670j>
- Turner, A.P.F., 2014. *Glucosensors and Enzymatic Biosensors* Glucosensors and Enzymatic Biosensors.
- Turner, R., 1998. Effect of intensive blood-glucose control with metformin on complications in overweight patients with type 2 diabetes (UKPDS 34). *Lancet*. [https://doi.org/10.1016/S0140-6736\(98\)07037-8](https://doi.org/10.1016/S0140-6736(98)07037-8)
- UK Prospective Diabetes Study Group, 1998. Effect of intensive blood-glucose control with metformin on complications in overweight patients with type 2 diabetes (UKPDS 34). UK Prospective Diabetes Study (UKPDS) Group. *Lancet*.
- Van Den Berghe, G., Wilmer, A., Hermans, G., Meersseman, W., Wouters, P.J., Milants, I., Van Wijngaerden, E., Bobbaers, H., Bouillon, R., 2006. Intensive insulin therapy in the medical ICU. *N. Engl. J. Med.* <https://doi.org/10.1056/NEJMoa052521>
- Vashist, S., 2013. *Continuous Glucose Monitoring Systems: A Review*. *Diagnostics*. <https://doi.org/10.3390/diagnostics3040385>

- Viet, N.X., Chikae, M., Ukita, Y., Takamura, Y., 2018. Enzyme-free glucose sensor based on micro-nano Dualporous gold-modified screen-printed carbon electrode. *Int. J. Electrochem. Sci.*
<https://doi.org/10.20964/2018.09.08>
- Wang, B., Zhang, J., Dong, S., 2000. Silica sol-gel composite film as an encapsulation matrix for the construction of an amperometric tyrosinase-based biosensor. *Biosens. Bioelectron.* [https://doi.org/10.1016/S0956-5663\(00\)00096-8](https://doi.org/10.1016/S0956-5663(00)00096-8)
- Wang, C., Chen, S., Xiang, Y., Li, W., Zhong, X., Che, X., Li, J., 2011. Glucose biosensor based on the highly efficient immobilization of glucose oxidase on Prussian blue-gold nanocomposite films. *J. Mol. Catal. B Enzym.*
<https://doi.org/10.1016/j.molcatb.2010.12.002>
- Wang, G., He, X., Wang, L., Gu, A., Huang, Y., Fang, B., Geng, B., Zhang, X., 2013. Non-enzymatic electrochemical sensing of glucose. *Microchim. Acta.*
<https://doi.org/10.1007/s00604-012-0923-1>
- Wang, H.C., Lee, A.R., 2015. Recent developments in blood glucose sensors. *J. Food Drug Anal.* <https://doi.org/10.1016/j.jfda.2014.12.001>
- Wang, J., 2001. Glucose biosensors: 40 Years of advances and challenges. *Electroanalysis.* [https://doi.org/10.1002/1521-4109\(200108\)13:12<983::aid-elan983>3.0.co;2-%23](https://doi.org/10.1002/1521-4109(200108)13:12<983::aid-elan983>3.0.co;2-%23)

- Wang, Linan, Tang, Y., Wang, Liu, Zhu, H., Meng, X., Chen, Y., Sun, Y., Yang, X.J., Wan, P., 2015. Fast conversion of redox couple on Ni(OH)₂/C nanocomposite electrode for high-performance nonenzymatic glucose sensor. *J. Solid State Electrochem.* <https://doi.org/10.1007/s10008-014-2689-3>
- Wang, R.T., Liu, E.E., Xu, A.F., Yang, L.W., Chen, J.Y., Xu, G., 2020. Ethylammonium lead iodide formation in MAPbI₃ precursor solutions by DMF decomposition and organic cation exchange reaction. *Crystals.* <https://doi.org/10.3390/cryst10030162>
- Wang, Y., Xu, Y., Luo, L., Ding, Y., Liu, X., Huang, A., 2010. A novel sensitive nonenzymatic glucose sensor based on perovskite LaNi_{0.5}Ti_{0.5}O₃-modified carbon paste electrode. *Sensors Actuators, B Chem.* <https://doi.org/10.1016/j.snb.2010.09.052>
- Wani, W.A., Prashar, S., Shreaz, S., Gómez-Ruiz, S., 2016. Nanostructured materials functionalized with metal complexes: In search of alternatives for administering anticancer metallodrugs. *Coord. Chem. Rev.* <https://doi.org/10.1016/j.ccr.2016.01.001>
- Whiting, D.R., Guariguata, L., Weil, C., Shaw, J., 2011. IDF Diabetes Atlas: Global estimates of the prevalence of diabetes for 2011 and 2030. *Diabetes Res. Clin. Pract.* <https://doi.org/10.1016/j.diabres.2011.10.029>

- Wilson, R., Elizabeth, Q., 2016. Glucose oxidase : An ideal enzyme Review article Glucose oxidase. *Biosens. t Biwlecrronia* 5663, 165–185.
[https://doi.org/10.1016/0956-5663\(92\)87013-F](https://doi.org/10.1016/0956-5663(92)87013-F)
- Wu, H.X., Cao, W.M., Li, Y., Liu, G., Wen, Y., Yang, H.F., Yang, S.P., 2010. In situ growth of copper nanoparticles on multiwalled carbon nanotubes and their application as non-enzymatic glucose sensor materials. *Electrochim. Acta*. <https://doi.org/10.1016/j.electacta.2010.02.017>
- Wu, W., Li, Y., Jin, J., Wu, H., Wang, S., Xia, Q., 2016. A novel nonenzymatic electrochemical sensor based on 3D flower-like Ni₇S₆ for hydrogen peroxide and glucose. *Sensors Actuators, B Chem*.
<https://doi.org/10.1016/j.snb.2016.04.006>
- Wu, Z.S., Zhou, G., Yin, L.C., Ren, W., Li, F., Cheng, H.M., 2012. Graphene/metal oxide composite electrode materials for energy storage. *Nano Energy*. <https://doi.org/10.1016/j.nanoen.2011.11.001>
- Xu, A.F., Wang, R.T., Yang, L.W., Liu, N., Chen, Q., Lapierre, R., Isik Goktas, N., Xu, G., 2019. Pyrrolidinium containing perovskites with thermal stability and water resistance for photovoltaics. *J. Mater. Chem. C*.
<https://doi.org/10.1039/c9tc02800e>
- Yadav, J., Rani, A., Singh, V., Murari, B.M., 2015. Prospects and limitations of non-invasive blood glucose monitoring using near-infrared spectroscopy.

Biomed. Signal Process. Control.

<https://doi.org/10.1016/j.bspc.2015.01.005>

Yang, H., Gao, G., Teng, F., Liu, W., Chen, S., Ge, Z., 2014. Nickel Hydroxide Nanoflowers for a Nonenzymatic Electrochemical Glucose Sensor. *J. Electrochem. Soc.* <https://doi.org/10.1149/2.0521410jes>

<https://doi.org/10.1149/2.0521410jes>

Yoo, E.H., Lee, S.Y., 2010. Glucose biosensors: An overview of use in clinical practice. *Sensors.* <https://doi.org/10.3390/s100504558>

Yoon, Y.S., Kim, J., Lee, K., Song, H., Yoo, K., Lee, G., Lee, J.B., 2011. A novel microneedle-based non- enzymatic glucose sensor for painless diabetes testing application, in: 2011 16th International Solid-State Sensors, Actuators and Microsystems Conference, TRANSDUCERS'11.

<https://doi.org/10.1109/TRANSDUCERS.2011.5969350>

Yu, J., Liu, S., Ju, H., 2003. Glucose sensor for flow injection analysis of serum glucose based on immobilization of glucose oxidase in titania sol-gel

membrane. *Biosens. Bioelectron.* [https://doi.org/10.1016/S0956-](https://doi.org/10.1016/S0956-5663(03)00199-4)

[5663\(03\)00199-4](https://doi.org/10.1016/S0956-5663(03)00199-4)

Yuan, J., Wang, K., Xia, X., 2005. Highly ordered platinum-nanotubule arrays for amperometric glucose sensing. *Adv. Funct. Mater.*

<https://doi.org/10.1002/adfm.200400321>

- Zang, G., Hao, W., Li, X., Huang, S., Gan, J., Luo, Z., Zhang, Y., 2018. Copper nanowires-MOFs-graphene oxide hybrid nanocomposite targeting glucose electro-oxidation in neutral medium. *Electrochim. Acta*.
<https://doi.org/10.1016/j.electacta.2018.05.016>
- Zayats, M., Katz, E., Willner, I., 2002. Electrical contacting of glucose oxidase by surface-reconstitution of the apo-protein on a relay-boronic acid-FAD cofactor monolayer. *J. Am. Chem. Soc.* 124, 2120–2121.
<https://doi.org/10.1021/ja025503e>
- Zhai, D., Liu, B., Shi, Y., Pan, L., Wang, Y., Li, W., Zhang, R., Yu, G., 2013. Highly sensitive glucose sensor based on pt nanoparticle/polyaniline hydrogel heterostructures. *ACS Nano*. <https://doi.org/10.1021/nn400482d>
- Zhang, C., Ni, H., Chen, R., Zhan, W., Zhang, B., Lei, R., Xiao, T., Zha, Y., 2015. Enzyme-free glucose sensing based on Fe_3O_4 nanorod arrays. *Microchim. Acta*. <https://doi.org/10.1007/s00604-015-1511-y>
- Zhang, R., Chen, W., 2017. Recent advances in graphene-based nanomaterials for fabricating electrochemical hydrogen peroxide sensors. *Biosens. Bioelectron.* <https://doi.org/10.1016/j.bios.2016.01.080>
- Zhang, S., Wang, N., Yu, H., Niu, Y., Sun, C., 2005. Covalent attachment of glucose oxidase to an Au electrode modified with gold nanoparticles for use

as glucose biosensor. *Bioelectrochemistry*.

<https://doi.org/10.1016/j.bioelechem.2004.12.002>

Zhang, W., Li, G., 2004. Third-Generation Biosensors Based on the Direct Electron Transfer of Proteins. *Anal. Sci.*

<https://doi.org/10.2116/analsci.20.603>

Zhang, X., Zhang, Z., Liao, Q., Liu, S., Kang, Z., Zhang, Y., 2016.

Nonenzymatic glucose sensor based on in situ reduction of Ni/NiO-graphene nanocomposite. *Sensors (Switzerland)* 16, 1–10.

<https://doi.org/10.3390/s16111791>

Zhao, C.X., Wang, K., Yan, H., Xu, G., 2011. Output current increase in alkaline glucose fuel cells. *J. Electrochem. Soc.* 158, 1055–1059.

<https://doi.org/10.1149/1.3596019>

Zhu, H., Li, L., Zhou, W., Shao, Z., Chen, X., 2016. Advances in non-enzymatic glucose sensors based on metal oxides. *J. Mater. Chem. B.*

<https://doi.org/10.1039/C6TB02037B>

Zhuang, Z., Su, X., Yuan, H., Sun, Q., Xiao, D., Choi, M.M.F., 2008. An improved sensitivity non-enzymatic glucose sensor based on a CuO

nanowire modified Cu electrode. *Analyst*. <https://doi.org/10.1039/b712970j>

Zhuo, Y., Chai, Y.Q., Yuan, R., Mao, L., Yuan, Y.L., Han, J., 2011. Glucose oxidase and ferrocene labels immobilized at Au/TiO₂ nanocomposites with

high load amount and activity for sensitive immunoelectrochemical
measurement of ProGRP biomarker. Biosens. Bioelectron.

<https://doi.org/10.1016/j.bios.2011.02.043>